Final Report to the Joint Fire Science Program
Project #11-1-5-13

Modeling Study of the Contribution of Fire Emissions on BC Concentrations and Deposition Rates

Author list:

[1]Serena H. Chung, [1]Brian K. Lamb, [1*]Farren Herron-Thorpe, [1†]Rodrigo Gonzalez-Abraham, [1]Vikram Ravi, [1]Tsengel Nergui, [1]Joseph K. Vaughan, [2]Narasimhan K. Larkin, [3]Tara M. Strand

[1]Washing State University
[2]U.S. Forest Service, Seattle, Washington
[2]Scion, NZ Crown Research Institute, Christchurch, New Zealand
[*]Now at Washington State Department of Ecology
[†]Now at Portland State University

Abstract

Regional air quality simulations were performed to evaluate the contributions of wildland fires to inter-annual variability of black carbon (BC) concentrations and to assess the contributions of wildfires vs. prescribed fires to BC concentrations and deposition rates to glacier areas and snow-covered surfaces in the western US.

Simulations for June-September of 1997-2005 indicated that monthly mean BC concentrations over most of the western US were significantly elevated by wildland fires for at least one month during this period. Wildland fires contributed greater than 50% of the monthly mean BC concentrations in Idaho, Montana, and northern Wyoming during August and September. The central and north central Idaho regions were most affected by wildland fires. Modeling results and observations from the IMPROVE network indicated that wildland fire emissions contributed significantly to the inter-annual variations in August-mean BC concentrations in Idaho, Montana, northern Wyoming, Utah Colorado, and the eastern Dakotas.

Simulations for the full year of 2011 indicated that the seasonal trend in relatively contributions of wild and prescribed fires to BC concentrations followed closely to the seasonal trend in their emissions: wildfires had the largest contributions during the summer while prescribed fires contributions were the most significant during the fall and early winter. In contrast, their relative contributions to BC deposition reflected other factors, including specific relationships of fire locations and wind directions relative to snowpack locations and the relative lofting heights of wildfires vs. prescribed burns. Non-wildland fire sources dominated annual total BC deposition rates to glacial areas, but monthly contributions during summer from wildfires and during fall and winter from prescribed fires can be significant (> 40%).

For BC deposition to snow-covered surfaces, prescribed fires in Washington, Oregon, Idaho, Wyoming, and Colorado were significant contributors (40% to more than 90%) in significant portions of these states during November. Prescribed fire contributions were also significant in central Colorado during December. These were the months when high emissions from prescribed fires coincided with the snow season. Because wildfires occurred predominantly during warmer months when the snow-covered areas were small, contributions from wildfires were generally negligible except for some small regions in October and May.
Because fire activities and snow amounts vary significantly from year to year, the analysis performed here should be extended to include more years.

1. Introduction

Increases in short-lived climate forcers such as aerosols have perturbed the Earth's radiative balance and may be contributing significantly to anthropogenic climate change (IPCC, 2007). These effects complicate our understanding of the climate impacts and changes expected from long-lived greenhouse gases (LLGHGs). Aerosols can cool the atmosphere by scattering incoming solar radiation back to space, or they can warm the atmosphere by absorbing solar radiation. Black carbon (BC) is the main aerosol component that absorbs solar radiation. Like other aerosol types, BC can also affect Earth's radiative balance indirectly by acting as cloud condensation nuclei, thereby impacting cloud formation and propagation. In addition, atmospheric warming by BC can inhibit the formation or cause evaporation of low-level clouds (Ackerman et al., 2000), thereby increasing the warming effect by allowing more radiation to reach the surface. Deposition of BC onto snow and ice surfaces further contributes to climate warming by decreasing surface albedo (Hansen and Nazarenko, 2004; Jacobson 2004; Qian et al., 2009). For these reasons, BC is increasingly recognized as an important contributor to global warming and regional climate change (Menon et al., 2002; Jacobson, 2004; Chung and Seinfeld, 2005; Bond ..Ramanathan and Carmichael, 2008). Reduction of BC emissions is a potential strategy for mitigating global warming (Jacobson, 2002; Bond, 2007) because it is emitted in large quantities and has a relatively short lifetime in the atmosphere in comparison to LLGHGs.

Evaluating the impact of BC emission reductions in the context of air pollution control and climate change mitigation requires several factors be considered. BC is co-emitted with organic carbon (OC), which contributes to total PM pollution and scatters light. The ratio of emitted BC and OC is important in determining the overall climate effects that would result due to BC emission controls because OC light scattering is estimated to cool the atmosphere (Chung and Seinfeld, 2002; Jacobson, 2002). In the case of fire emissions, BC is also co-emitted with significant quantities of volatile organic compounds (VOCs) that can form secondary organic aerosol (SOA), a form of OC that also scatters light and thus offsets warming by BC. Finally, coating by OC and other aerosol components, such as sulfate and nitrate, increases the absorption efficiency of BC. Thus, a full chemistry model that simulates all aerosol components is necessary to evaluate the impact of BC from fires on air quality and on the climate system.

There is strong evidence that climate change has caused an increase in wildfire activity. Westerling et al. (2006) found that the observed increase in large forest wildfires in the western US since the mid-1980s is associated with unusually warm springs resulting in early spring snowmelt and longer summer dry seasons. Several studies have predicted increased wildfire risk and area burned for various future climate-warming scenarios (e.g., Barbero et al., 2015; Flannigan et al., 2009). In addition, Spracklen et al. (2009) estimated that increased wildfire emissions will increase summertime OC and BC concentrations over the western US by 30% and 20%, respectively, from 2000 to 2050 under the IPCC Special Report on Emissions Scenarios (SRES) A2 scenario (Nakićenović 2000). Chen et al., (2009a) reported a 25% increase in VOC and CO emissions from wildfires in western US in the 2050s for the A2 scenario relative to the 1990-1999 decade.

Wildland fires are a major source of particulate emissions, including BC. In combination with other emissions, these BC and particulate emissions can directly lead to air quality degradation, both locally and regionally. Assessing the effects of fire BC and particulate emissions on the overall climate system requires placing fire in a larger context of different emissions sources. Due to the highly variable nature of wildfires, both in fire occurrences on the landscape and the high spatial and temporal variability of fuels, consumption, and emissions, the impact of wildfire

emissions varies significantly over the period of the wildfire season as well as inter-annually. In addition, contribution of fire emissions to BC is expected to increase in the future due to the combination of expected reduction in non-biomass burning anthropogenic emissions and an increase in wildfire activity due to a warmer climate. Thus, a robust analysis on the role of BC from fire emissions on air quality and climate necessitates a comprehensive, multi-scale study of all fire-related pollutants and other emission sources spanning multiple years of fire data and weather conditions while incorporating extensive evaluation of model results using observational data.

This study addressed the following key questions using a multi-pollutant regional air-quality modeling system:

1. What are the contributions to ambient BC from prescribed fire and wildfire in the western US?
2. How do these contributions vary seasonally and regionally?
3. What are the contributions from fires to deposition rates of BC onto glaciers and snow-covered surfaces?

2. Methodology

To answer the key questions of this work, we used a regional air quality modeling framework (Figure 1). The framework consisted of a weather model, inventories of emissions including prescribed and wildfire emissions, several emission processors required to integrate emissions inventories with air quality simulations, and a comprehensive full-photochemical air quality model. These are described in detail below.

Several simulations were done both regionally and across the contiguous lower 48 United States (CONUS). These include:

- 1997-2005 Wildfire Season (June-September) CONUS simulations
- 2011 Full Year Western U.S. simulations

Table 1 lists the simulations performed; Table 2 summarizes the configurations of the simulations.

Table 1. WRF/CMAQ simulations performed for this study

Set	Domain	Grid Cell	Time Period	Fire Emission
36-km	CONUS	36 km x 36 km	1997-2005; Jun-Sep	BLM[1]+BlueSky[2]
				None
12-km	Western US	12 km x 12 km	Jan-Dec, 2011	Full NEI[3] 2011 with all fires
				Partial* NEI 2011 with all fires
				Partial[4] NEI 2011 with wildfires but no prescribed forest fires
				Partial[4] NEI 2011 with no wildland fires

[1]Bureau of Land Management
[2]BlueSky Modeling Framework
[3]National Emissions Inventory
[4]NEI 2011 excluding point source emissions in the US.

Table 2. Configurations of modeling system

	36-km Simulation	12-km Simulation
Time Period	1997-2005; Jun-Sep	Jan-Dec, 2011
Initial and Boundary Dynamical Conditions	DOE/NCEP R-2	NARR
SST	NOAA OI v2	RTG_SST_HR
WRF ***Shortwave Radiation*** ***Longwave Radiation*** ***Microphysics*** ***Cumulus Param.*** ***Land Use Scheme*** ***Surface Layer Scheme*** ***PBL Scheme***	Version 3.2.1 CAM CAM WSM 5-class Kain-Fritsch NOAH Monin-Obukhov YSU	Version 3.5.1 RRTMG RRTMG Thompson New SAS NOAH Monin-Obukhov YSU
Fire Emissions ***Plume-rise***	BLM/BlueSky v3.3 WRAP	NEI 2011 (BlueSky v3.5) CMAQ inline
Anthropogenic Emissions	NEI 2002	NEI 2011
Biogenic Emissions	MEGANv2.04	BEIS v3.14
Chemical Boundary Conditions	MOZART-4 2009	
CMAQ ***Gas-phase mechanism*** ***Aerosol module***	Version 4.7.1 SAPRC99 AE5_AQ	Version 5.0.2 CBO5 AE6_AQ

2.1 Regional Air Quality Modeling Framework

To answer the key questions of this work, we used the WRF-BlueSky-SMOKE-CMAQ regional air quality modeling framework (Figure 1). The modeling framework was a combination of WRF (Weather Research and Forecasting) (Skamarock et al., 2008) for meteorology, SMOKE for emissions processing, and CMAQ (Community Multi-scale Air Quality) (Byun and Schere, 2006) for chemistry and transport. The results of WRF were processed through MCIP (Meteorology-Chemistry Interface Processor; Otte and Pleim, 2010) for analysis and to produce necessary files necessary for subsequent chemical transport model simulations using CMAQ. The BlueSky Framework (Larkin et al., 2009) with the FCCS, CONSUME 3.0, FEPS, and WRAP modules was used to for fire emissions. Table 1 lists the simulations performed for this project using the modeling framework shown in Figure 1;

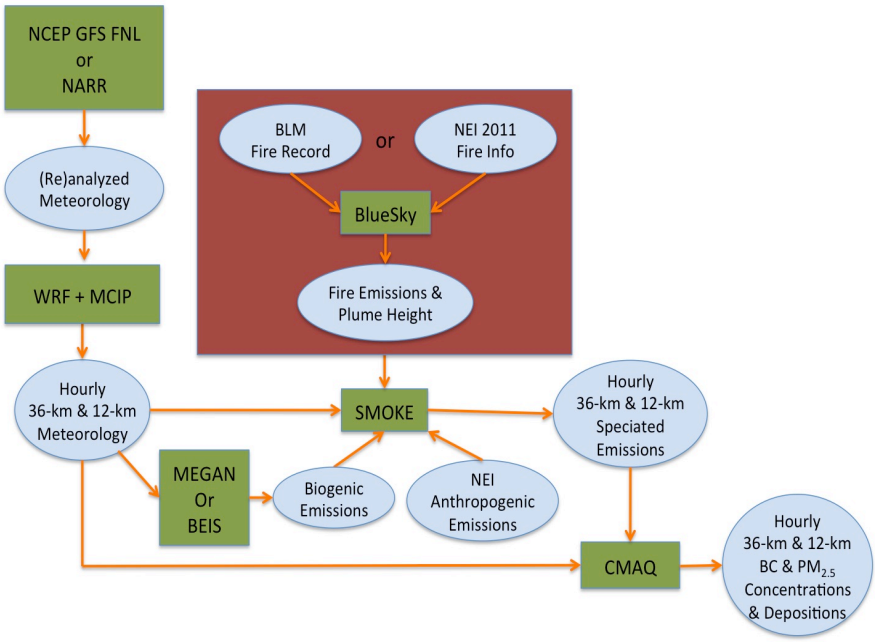

Figure 1. WRF-BlueSky-SMOKE-CMAQ regional air quality modeling framework used for this study

Table 2 summarizes the configurations of the simulations. Evaluations of the model results are provided in Appendix A.

2.2 Simulation Period #1 – 1997-2005 June-September CONUS

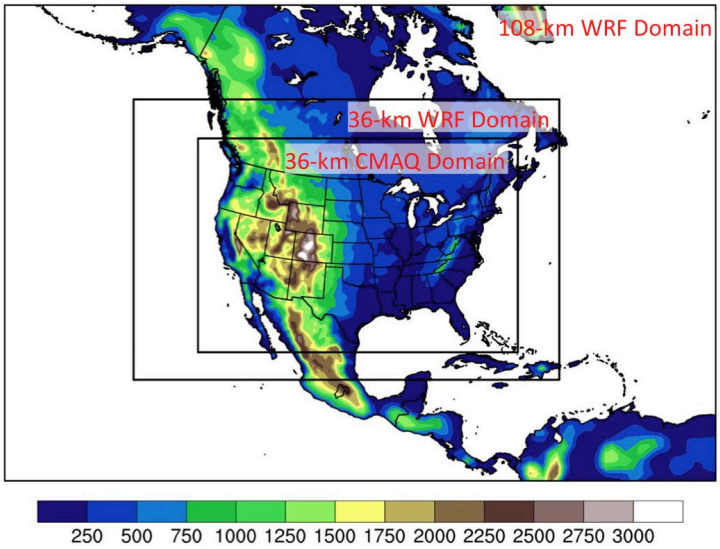

Figure 2. Terrain height (m) for the nested 108-km and 36-km WRF and 36-km CMAQ simulation domains used for the 1997-2005 June-September simulations.

2.2.2 Model Configuration

The contiguous US (CONUS) simulations were performed for June-September of 1997-2005 to evaluate inter-annual variability of wildfire emissions in the western US on atmospheric BC concentrations. Summertime simulations were selected because inter-annual variability is driven mostly by variability in wildfires, which occurs predominantly during summer in the western US. We chose 1997-2005 so that we can cover inter-annual variability associated with the El Niño Southern Oscillation (ENSO) cycle, an important driver of forest fire regimes (Swetnam and Betancourt, 1990). The most notable ENSO cycle during 1997-2005 is the 1997-1998 El Niño and 1999-2001 La Niña events. The 1997-1998 El Niño was one of the biggest events recorded in history (NOAA's Climate Prediction Center (NOAA/CPC); http://www.cpc.ncep.noaa.gov/products/analysis_monitoring/ensostuff/ensoyears.shtml).

For the 1997-2005 summertime 36-km CMAQ simulations, nested 108-km and 36-km WRFv3.2.1 simulations were performed (domains shown in Figure 2), using the initial and lateral boundary conditions interpolated from the National Centers for Environmental Prediction-Department of Energy Reanalysis 2 (NCEP-DOE R-2) results (Kanamitsu et al. 2002), with the lateral boundary conditions updated every six hours. Analysis nudging was applied to the 108-km domain. Sea surface temperature (SST) was updated weekly using the NOAA optimum interpolation (OI) SST version 2 (Reynolds et al. 2002). The National Emission Inventory (NEI) 2002 was used for anthropogenic emissions. MEGAN (Model of Emissions of Gases and Aerosols from Nature) (Guenther et al., 2006) v2.04 was used to model biogenic emissions, using modeled WRF meteorological results as input. Because long-range transport of BC and $PM_{2.5}$ precursors is typically not significant for regional air quality in the US, the specific

boundary condition used is not critical to the study. Monthly-mean chemical fields from MOZART-4 global climate model results (Emmons et al., 2010) for June-September 2009 were used as chemical boundary conditions.

2.2.1 Wildland Fire Emission Inventory for 1997-2005

The 1997-2005 summertime 36-km CMAQ simulations used historical fire records collected by the Bureau of Land Management (BLM) (http://capita.wustl.edu/fsan/FedFireHist.htm); they contain fire location and size for wild, managed, and prescribed fires done on public lands (Figure 3a). BlueSky was run with the 1-km Fuel Characteristic Classification System (FCCS) v1 fuel map (McKenzie et al., 2007, http://www.fs.fed.us/pnw/fera/fccs/maps.shtml), CONSUME v3 (Pritchard et al, 2006) for consumption, and Fire Emissions Production Simulator (FEPS) (Anderson et al. 2004) for time rate and emissions, and Western Regional Air Partnership (WRAP) plume rise to produce hourly $PM_{2.5}$, PM_{10}, CO, NH_3, NO_X ($NO+NO_2$), SO_2, and volatile organic compound (VOC) emissions in SMOKE-file format; monthly $PM_{2.5}$ fire emissions are summarized in Figure 3b. SMOKE was then used to speciate $PM_{2.5}$, NO_X, and VOC and to produce three-dimensional CMAQ-ready emission files with the vertical profiles based on WRAP plume rise results, which did not consider modeled meteorological conditions. In SMOKE, 16% and 77% of $PM_{2.5}$ of these emissions were split into BC and organic aerosol, respectively, following Chen et al. (2008). Because wildfires are predominant in the western US, the evaluation focused on the western US.

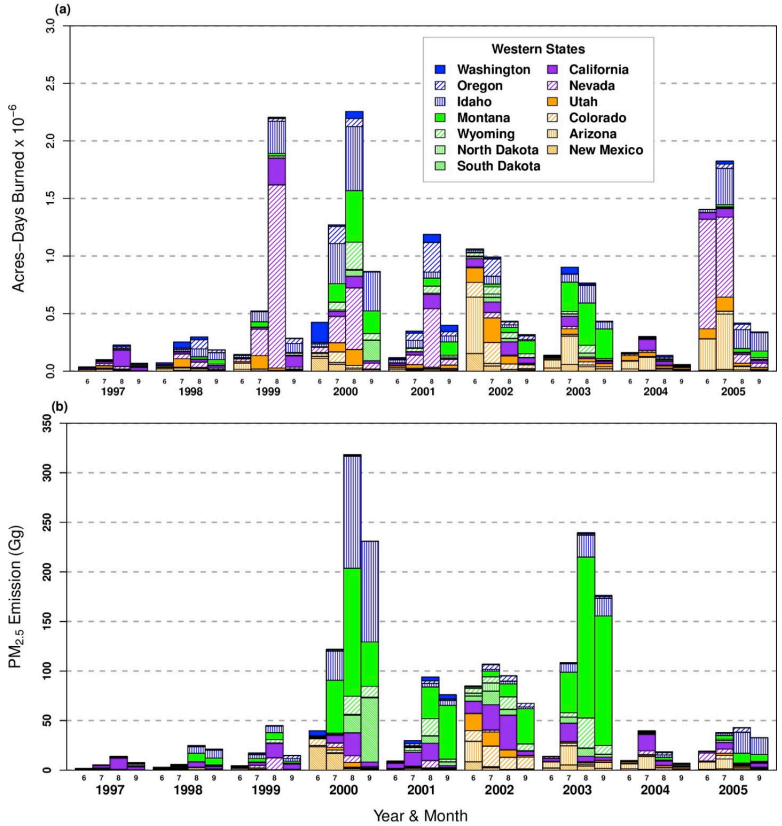

Figure 3. (a) Monthly total acres-days burned from Federal Fire History Internet Map Service provided by the Bureau of Land Management (BLM) (http://capita.wustl.edu/fsan/FedFireHist.htm). (b) Monthly $PM_{2.5}$ emission simulated by BlueSky v3.3 based on the BLM fire records.

2.3 Simulation Period #2 – 2011 Western U.S.

2.3.1 Model Configuration

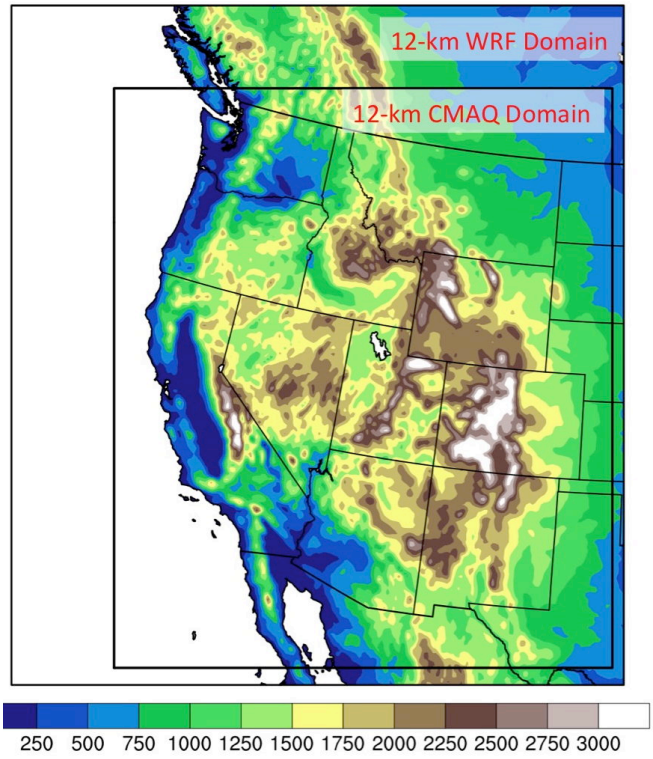

Figure 4. Terrain height (m) for WRF and CMAQ modeling domains used for the 2011 simulations.

Figure 4 shows the WRF and CMAQ domains for the 2011 12-km western US simulations. For the WRFv3.5.1 simulation, the initial and lateral boundary conditions were interpolated from the North American Regional Reanalysis (NARR; Mesinger et al., 2006), with the lateral boundary conditions updated every three hours. SST was updated daily using the NOAA's 0.083 degrees by 0.083 degrees real-time, global SST analysis products (RTG_SST_HR) (http://polar.ncep.noaa.gov/sst/ophi/). Monthly-mean chemical fields from MOZART-4 global climate model results (Emmons et al., 2010) for 2009 were used as chemical boundary conditions. All emissions were based on NEI 2011v1 2011ec_v6_11f platform (ftp://ftp.epa.gov/EmisInventory/2011v6/v1platform/2011emissions/). NEI 2011 includes anthropogenic, biogenic, agricultural burning (crop residual burning), and wildland fire emissions (see below). Biogenic emissions are based on BEIS (Biogenic Emission Inventory System) (Vukovich and Pierce, 2002) v3.14.

2.3.2 Wildland Fire Emission Inventory for 2011

The wildland fire emissions inventory used for the 2011 simulation is from the national scale processing developed as part of the 2011 Environmental Protection Agency's (EPA) National Emissions Inventory and performed by the U.S. Forest Service AirFire Team and Sonoma Technology in collaboration with the EPA (Raffuse et al, in review). The emissions inventory includes both prescribed burns and wildfires derived from multiple fire reporting and satellite fire detection systems. Overall six national databases plus local data from 23 states were incorporated into the inventory making it the most complete fire emissions database of its kind. Fire emissions include very small prescribed burns and wildfires as the data are available via local databases and/or as the fires are detected by satellites. Data for larger fires are more complete due to both greater detection likelihoods and more stringent reporting requirements. National databases used include the Incident Command Summary (ICS-209) reports, fire perimeters from the Geospatial Multi-Agency Coordination (GeoMAC), the federal prescribed fire databases from the Department of Interior (National Fire Plan Operations and Reporting System – NFPORS) and the U.S. Forest Service (Forest Service ACtivity Tracking System – FACTS), and the National Association of State Foresters (NASF). Additionally satellite detections were incorporated from the National Oceanic and Atmospheric Administration's Hazard Mapping System (HMS) that combines fire detections from multiple geostationary and polar orbiting satellite sensors. State data were also incorporated, including through the multi-

state Fire Emissions Tracking System (FETS) run by the Western Regional Air Partnership and by individual state submissions.

Fire occurrence data were combined using the SmartFire fire information system, and emissions were computed using the BlueSky Modeling Framework (Larkin et al. 2009). The specific modeling pathway utilized included fuels data from the 1-km FCCS revised fuels map (McKenzie et al., 2007, http://www.fs.fed.us/pnw/fera/fccs/maps.shtml); consumption calculations via the CONSUME v4 model (Pritchard et al, 2006); and emission speciations via the FEPS (Anderson et al. 2004). Black carbon emissions are computed as proportional to overall $PM_{2.5}$ emissions (Larkin et al, 2014) using the ratio in SMOKE. SMOKE speciates $PM_{2.5}$ to 9.5% and 10.9% BC for wild and prescribed fires, respectively. Monthly total $PM_{2.5}$ emissions by states in the western US are shown in Figure 5.

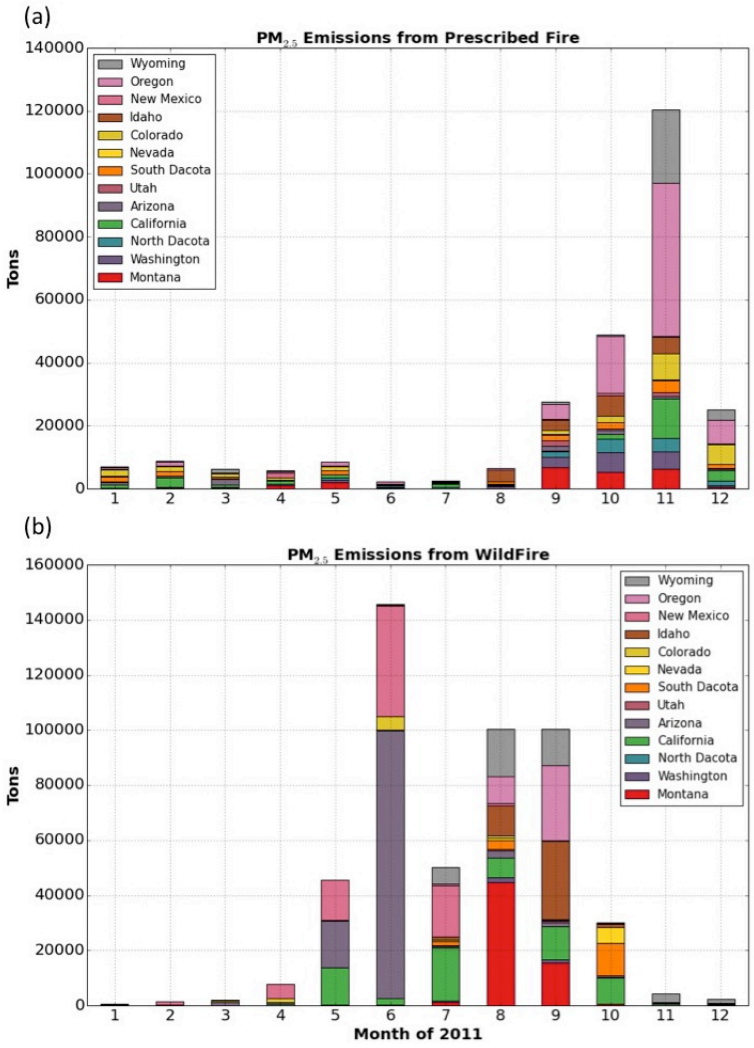

Figure 5. Monthly total $PM_{2.5}$ emissions by state for (a) prescribed fires and (b) wildfires from NEI 2011. SMOKE speciates $PM_{2.5}$ to 9.5% and 10.9% BC for wild and prescribed fires, respectively.

3. Key Findings

3.1 Wildland Fire Contributions to BC Concentrations during 1997-2005

- BC concentrations in most of the western US were significantly elevated by wildland fires at least one time in each state during the 1997-2005 period.
- Wildland fires contributed to greater than 50% of the monthly mean BC concentrations in Idaho, Montana, and northern Wyoming during August and September.
- The BC concentrations in the central and north central Idaho regions were most strongly influenced by wildland fires.
- Wildland fire emissions contributed significantly to the inter-annual variations in August-mean BC concentrations in Idaho, Montana, northern Wyoming, Utah Colorado, and eastern Dakotas.

Monthly mean BC concentrations from the 36-km CMAQ simulations for June-September of 1997-2005 were analyzed for contributions of wildland fires to ambient BC concentrations and their inter-annual variability. Figure 6 shows the observed and modeled monthly mean BC concentrations by year at 103 IMPROVE sites in the western US; the results were averaged by regions similar to those defined in Jaffe et al. (2008). Note that observational data were not available for all sites for the entire simulation period; model results shown in Figure 6 are only for the dates and sites for which IMPROVE data were available. In general, modeled BC concentrations without wildland fire emissions were much lower than the observed and showed small inter-annual variations. Without wildland fire emissions, BC emissions were assumed constant (NEI 2002) for all years and the only difference between the different years was meteorology, resulting in very small inter-annual variability in monthly BC concentrations when averaged over large regions. Because El Niño's impact on meteorology in the western US predominantly occurs during winter and spring (Rasmusson and Wallace 1983), the 1997-1998 El Niño event, which was the strongest event on record, did not influence modeled BC concentrations during June-September at IMPROVE sites when wildland fire emissions were not included in the simulation.

Observed and modeled results shown in Figure 6 indicate that wildland fire emissions contributed significantly to the inter-annual variations in monthly mean BC concentrations in Region 1 (Idaho, western Montana, and northwestern Wyoming) for July and August, Region 2 (Utah and Colorado) for August, and Region 6 (eastern Montana, northeastern Wyoming, and eastern Dakotas) for July and August. In these cases, modeled and observed monthly BC concentrations were ~1.5 to 3 times higher in 2000 and/or 2003 than the average of 1997-2005. July and August of 2000 and 2003 were among the months with the highest wildland fire emissions in Idaho, Montana, and Wyoming during the 1997-2005 period according to the BLM historical fire records and BlueSky (Figure 3). The model results also suggested that wildland fire emissions contributed to large inter-annual variations in Region 1 for September, Region 2 for June and July, Region 3 (Arizona and New Mexico) for June and July, Region 4 (California) for June and July, and Region 6 for September; however, for these cases the observed concentrations and inter-annual variations were much lower than modeled. Observations in Region 5 (Washington and Oregon) exhibited large inter-annual variations that were suggestive of fire impacts; however, the BLM historical fire records indicated relatively few fires burned in these regions during 1997-2005 and the modeled fire contributions to monthly BC concentrations were small (Figure 6q-t).

IMPROVE sites were sparse, especially during the early part of the simulation period, and therefore were not necessarily representative of the whole western US. Figure 7 shows the spatial maps of monthly mean results averaged over the 1997-2005 period as well as the maximums of the monthly means in each grid cell. Averaged over the 1997-1995 period for most of the western US, wildland fires contributed to less than 30% (less than 0.03 $\mu g\ m^{-3}$) of the modeled monthly-mean total BC concentrations (first two columns of Figure 7) with anthropogenic sources contributing the remainder. However, Idaho, Montana, and northern Wyoming were strongly affected by wildland fires. In these regions, wildland fires contributed to greater than 50% of the average total monthly mean BC concentrations for July, August, and September (Figure 7e,h,k). In central and north central Idaho, the contributions were almost 5 $\mu g\ m^{-3}$ (Figure 7g,j) and as high as 84% of the total (Figure 7h,k) on average for August and September.

The third and fourth columns of Figure 7 show the maximum monthly-mean values in each grid cell during 1997-2005 to highlight the biggest impact by wildland fires for any given region during this period. Most of the western US were significantly impacted by wildland fires at some point during this period, with wildland fire emissions contributing to great than 80% of the monthly total BC concentration for at least one month.

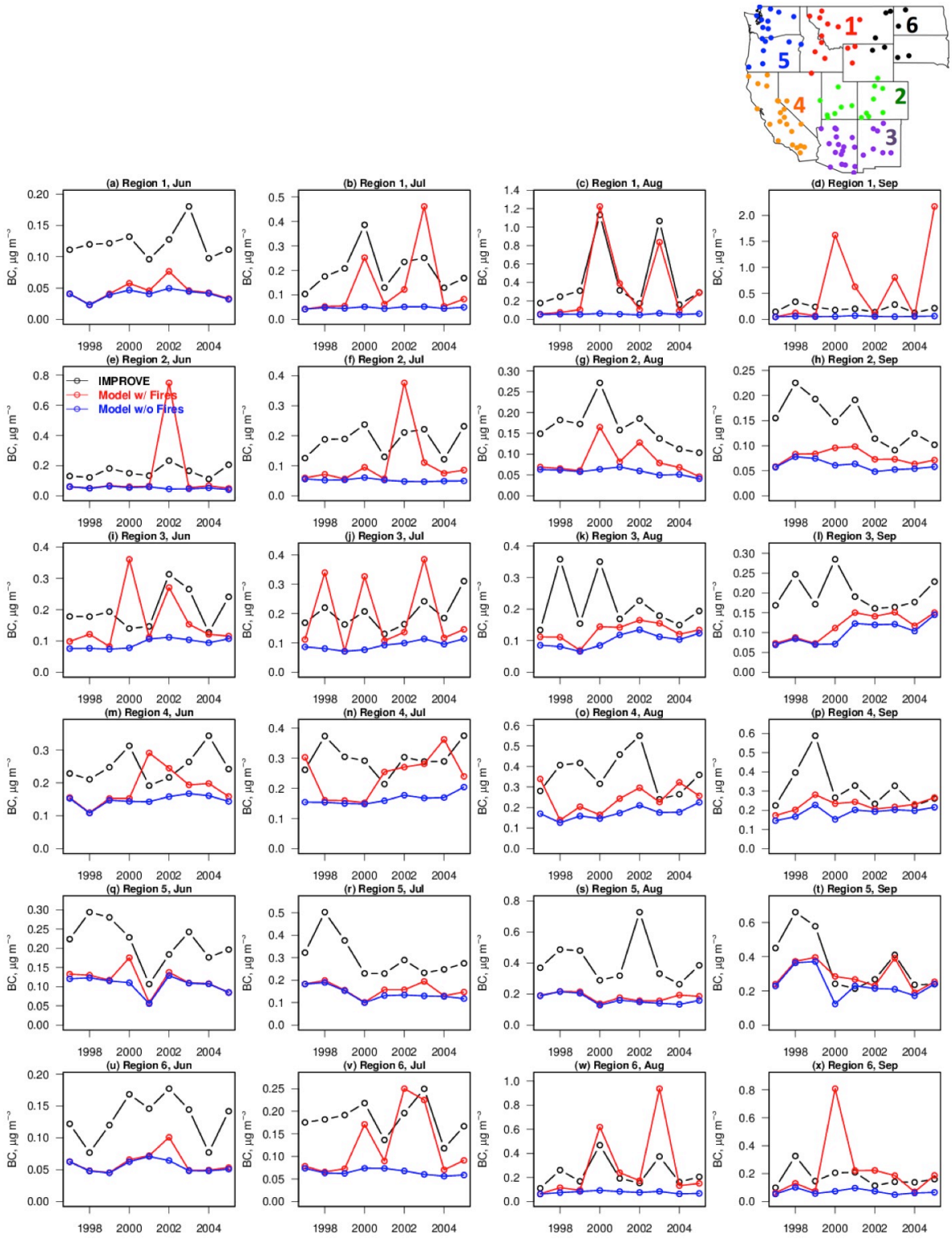

Figure 6. Observed and modeled monthly mean BC concentrations by year at 103 IMPROVE sites, which are aggregated by region. Left the right: June to September; top to bottom: Region 1 to Region 6. The regions are similar to those in Jaffe et al. (2008). Note the vertical scales are different among the graphs.

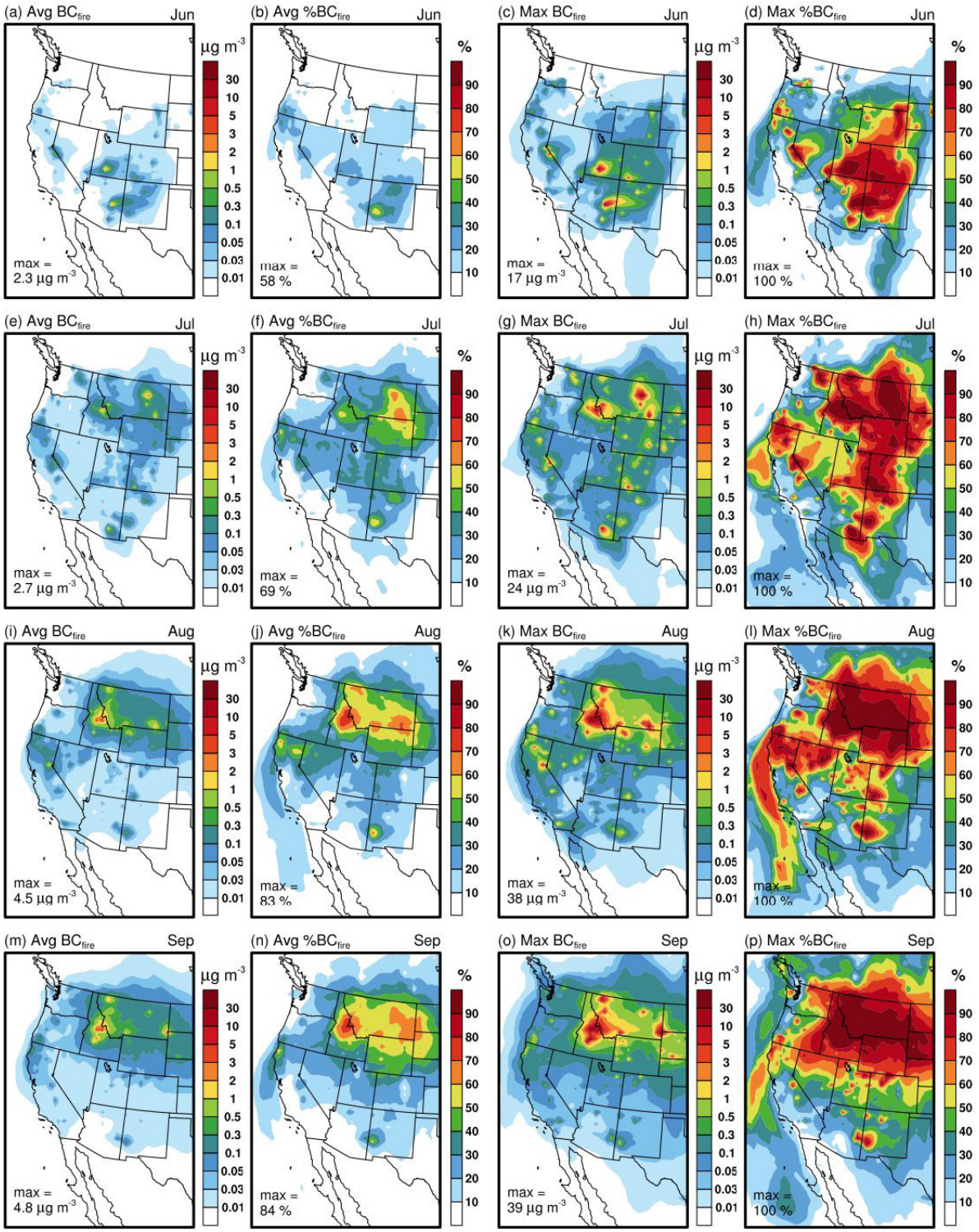

Figure 7. Contributions of fires to monthly mean BC concentrations based on averages or maximums of monthly mean model results during 1997-2005. Left to right: average values of monthly mean BC concentrations from fires, average values of monthly mean percent BC contribution due to fires, maximum values of monthly mean due to fires, and maximum values of percent monthly mean BC concentrations due to fires; top to bottom: June, July, August, and September.

3.2 Contributions of Wild and Prescribed Fires in 2011

- While seasonal trends in wildfire and prescribed burning contributions to ambient BC concentrations followed their overall emission trends, their contributions to BC deposition did not.

BC concentrations were analyzed separately from BC deposition. Overall wildfire and prescribed burning contributions to ambient BC concentrations (figure not shown) closely followed their relative contributions to BC emissions within the inventory. Their relative contributions to BC deposition reflected other factors including specific relationships of fire locations and wind directions relative to snowpack locations and the relative lofting heights of wildfires vs. prescribed burns.

3.2.1 Deposition to Glacier Areas in 2011

- Non-wildland fire sources dominated annual BC deposition rates to glacial areas, though monthly contributions during summer from wildfires and during fall and winter from prescribed fires can be significant.
- Contributions of prescribed fires to annual BC deposition to glacier areas were greater than those of wildfires.

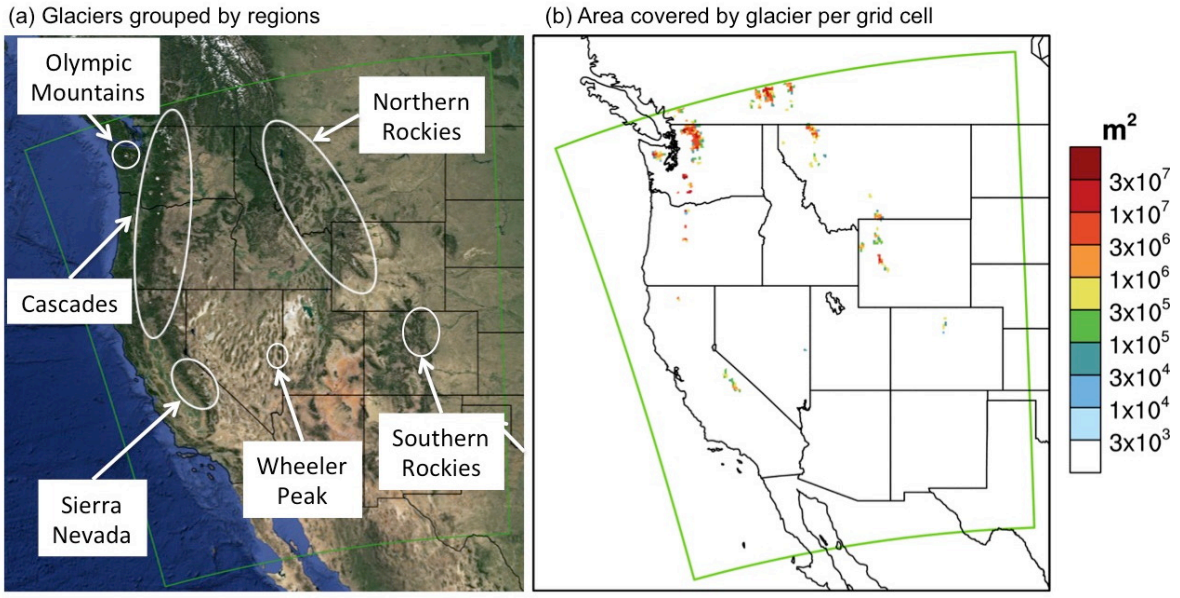

Figure 8. a) Regions of glaciers in the western US used in the analysis; b) area (m^2) covered by glacier mapped to CMAQ 12-km x 12-km CMAQ grid cells based on the GLIMS (Global Land and Ice Measurements from Space) Glacier Database (GLIMS and NSIDC, 2005). Light green lines in both figures indicate the CMAQ simulation domain.

Monthly and annual deposition rates of BC from the 2011 western US CMAQ simulation were analyzed. Figure 8 shows the glaciers in the western US according to the GLIMS (Global Land and Ice Measurements from Space) Glacier Database (GLIMS and NSIDC, 2005). The glaciers were grouped into seven areas for the analysis. Note that the glacier patches are smaller than the model grid cells (144 km^2 each); in calculating the deposition rates onto the glacier areas, we assumed that deposition rates were uniform within each grid cell. Glaciers in the modeling

domain but outside of US (northern Cascades and northern Rockies in Canada) were not considered in the analysis. The results are summarized in Figure 10 and Table 3.

Table 3. 2011 annual deposition rates of BC to seven glacier areas shown in Figure 8.

	Total	**Wildfires**		**Prescribed Fires**	
	kg/ha	kg/ha	% of total	kg/ha	% of total
Cascades	0.66	0.006	1%	0.084	13%
Northern Rockies	0.48	0.032	7%	0.079	16%
Olympic	0.46	0.002	0.4%	0.035	8%
Sierra Nevada	0.33	0.075	23%	0.017	5%
Southern Rockies	0.54	0.038	7%	0.111	21%
Wheeler Peak	0.13	0.008	6%	0.002	2%

Of the glacier areas analyzed, non-wildland fire sources dominated the annual total BC deposition rates (Figure 9 and Table 3). On an annual basis, wildland fires contributed greater than 20% of total BC deposition only in the northern Rocky (23%), Sierra Nevada (28%), and the southern Rocky (28%) glacier areas, with prescribed fires contributing to most of the wildland fire portion in the northern Rocky (16% of total) and southern Rocky (21% of total) areas. The glacier area with the highest annual total BC deposition rate was the Cascades at 0.66 kg/ha, with small contributions of 1% and 13% for wild and prescribed fires, respectively. Wheeler Peak had the lowest annual total BC deposition rate a 0.13 kg/ha, with very small contributions of 6% and 2% for wild and prescribed fires, respectively. The Sierra Nevada area had the greatest relative contribution from wildfires, with wild and prescribed fires contributing 23% and 3%, respectively, to the total rate of 0.33 kg/ha.

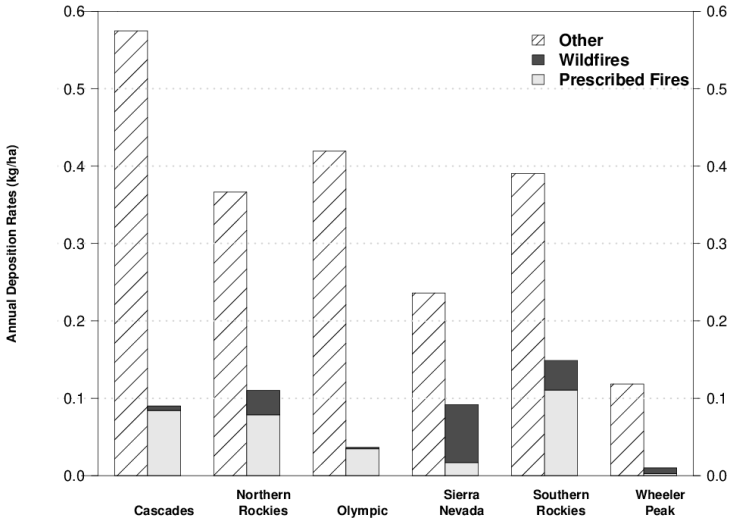

Figure 9. Annual BC deposition rates to seven glacier areas shown in Figure 8.

Figure 10 shows monthly total BC deposition rates to the glacier areas and the contribution from wild and prescribed fires. Figure 10a-c indicates that for all glacier areas except for the Rockies, sources other than wildland fires dominated BC deposition in the first half of the year. For glacier areas in the Cascades and the Olympic mountains, BC deposition rates peaked in March and November, with March being dominated by anthropogenic sources and significant contributions (45% for the Cascades and 54% for Olympic mountains) from prescribed fires in November (Figure 10ac). Total BC deposition rates also peaked in November in the southern Rockies, with 61% from prescribed fires (Figure 10e). For the northern Rockies in September, wildfires contributed a large portion of BC depositions on a percentage basis (59%), but the total BC deposition rates were small compared to other times of the year (Figure 10b). BC deposition rates in the Sierra Nevada peaked in July, and 65% was from wildfires (Figure 10d). For Wheeler Peak, wildland fire contributions occurred

predominantly in July and September, while prescribed fire contributions occurred predominantly in December (Figure 10f); as noted earlier, Wheeler Peak had the lowest annual BC deposition and the smallest contribution from wildland fires.

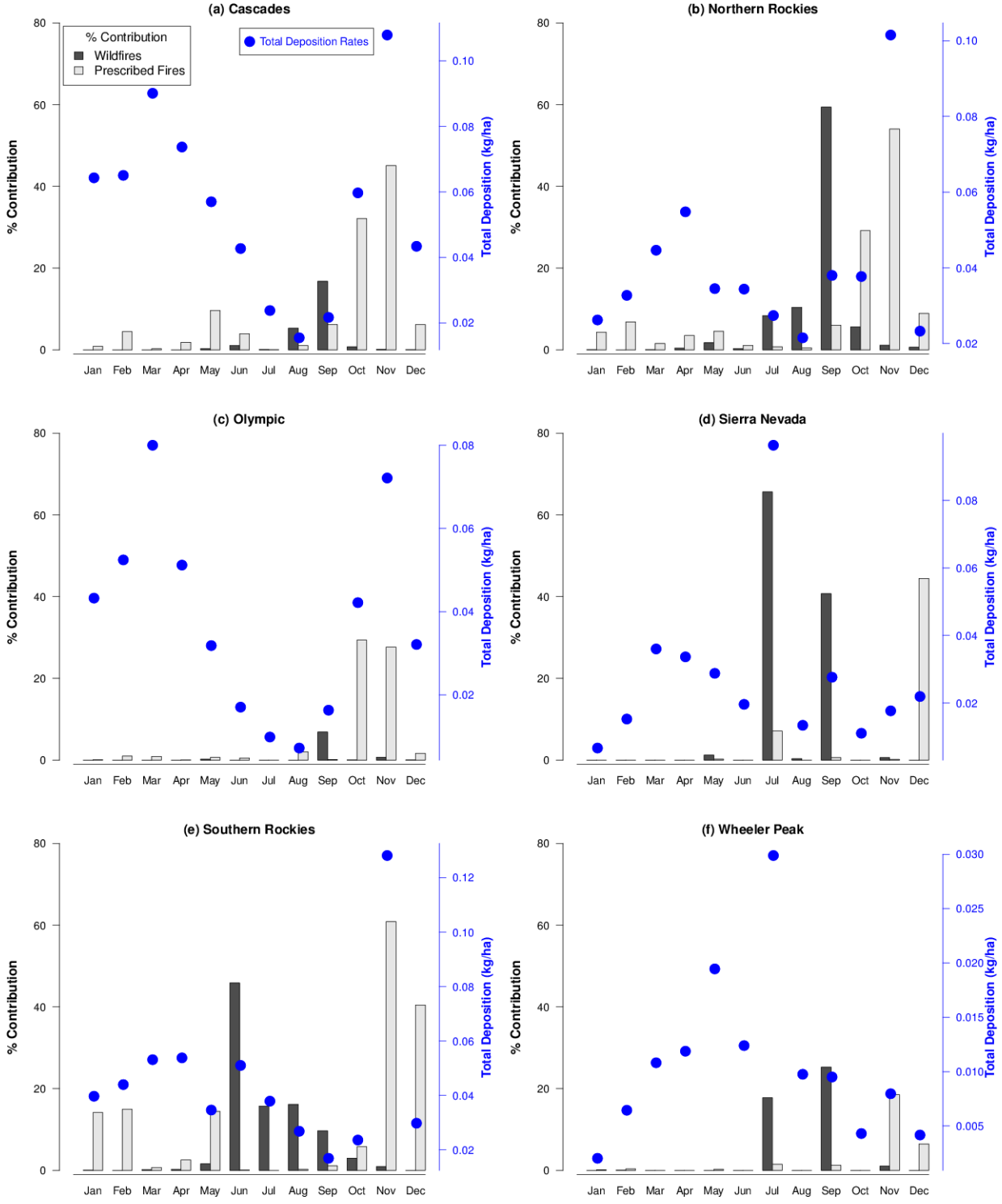

Figure 10. Monthly total black carbon deposition rates (blue dots and right axis) and contribution of wildfires and prescribe fires (gray bars and left axis) to glaciers areas as defined in Figure 8.

3.2.2 Deposition to Snow-Covered Areas in 2011

- Except for October and May, contributions of wildfires to BC deposition onto snow-covered surfaces were generally negligible because of a smaller snowpack during the summer months.
- Prescribed fires in Washington, Oregon, Idaho, Wyoming, and Colorado were significant contributors to BC deposition onto snow-covered surfaces in significant portions of these states during November.

Monthly deposition rates of BC from the 2011 western US CMAQ simulation were also analyzed for contribution to snow covered surfaces. To determine which modeled grid cells were covered by snow, we used snow depth data from NOAA National Weather Service's National Operational Hydrologic Remote Sensing Center (NOHRSC) Snow Data Assimilation System (SNODAS) Data Products (NOHRSC, 2004). SNODAS is modeling and data assimilation system designed to provide the best estimates of snow cover data. It integrates snow data from satellite, airborne and ground measurements with model estimates of snow cover (Carroll et al. 2001). Using the SNODAS snow depth data avoided the errors in snow predictions from the WRF simulations. Daily 30-arcsec SNODAS snow depth data for 2011 were aggregated to ¼-degree data using the Polaris website of the National Snow and Ice Data Center (NSIDC) (http://nsidc.org/data/polaris/). Daily ¼-degree data were then averaged to monthly mean values and mapped to 12 km x 12 km model grid cells. Figure 11 to Figure 13 show the modeled BC deposition rates and percent contribution from wild and prescribed fires for grid cells with monthly-mean snow depths greater than 3 cm for winter and spring months plus October and November.

In general the largest BC deposition rates occurred near urban areas and were dominated by anthropogenic sources. However, a major exception was during November, when prescribed fires from Washington, Oregon, Idaho, Wyoming, and Colorado contributed 40% to greater than 90% of the BC deposition to snow-covered surfaces in significant portions of these states (Figure 13f). Another notable exception was in central Colorado, where prescribed fire contributions reached ~80% in December (Figure 11i). In October, prescribed fires contributed up to 60% of the total BC deposition in central Idaho and less 10% in the rest of the Rockies (Figure 13c). These contributions reflected the high emission rates from prescribed fires during these months (Figure 5) coinciding with the snow season. During spring (March, April, and May) contributions from prescribed fires were generally less than 10% (Figure 11c,f,i). During May, prescribed fire contributions were concentrated in the Rockies, with contributions up to ~80% in Colorado and generally less than 10% in the Northern Rockies.

Because wildfires were predominantly occurred during warmer months when there were little or no snow, their contributions to total BC deposition onto snow-covered surfaces were generally negligible. During winter (January, February, and December), wildfire contributions to BC deposition rates in snow-covered regions were negligible (< 1% over much the region) (Figure 11b,e,f) except for a very small area in southwestern North Dakota where contributions from wildfires reached ~30% in January (Figure 11b), though the magnitude of total BC deposition rate was small (<30 g/ha; Figure 11a). During spring contributions from wildfires were also negligible (Figure 12b,e,h). Wildfires' contributions to BC deposition in snow-covered areas were highest in October, with contributions of up to 60% in central Idaho and greater than 90% in the border areas of Idaho and Nevada (Figure 13b).

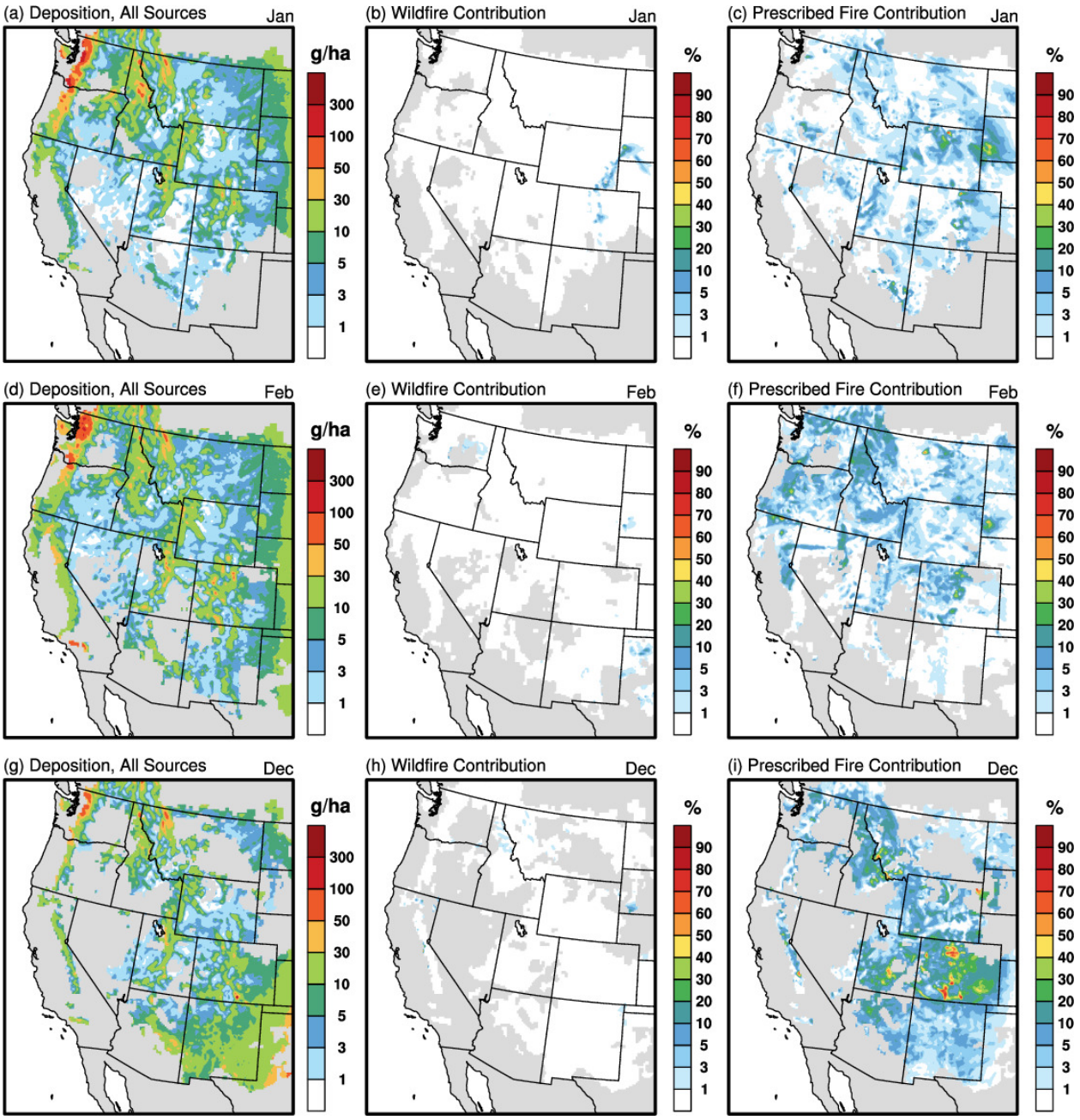

Figure 11. BC deposition for winter: monthly total from all sources (left panel) and percent contribution from wildfires (middle pane) and prescribed fires (right panel) for January (top panel), February (middle panel), and December (bottom panel) of 2011. Gray color indicates monthly-mean snow depths were less than 3 cm or snow depth data were missing in the SNODAS database.

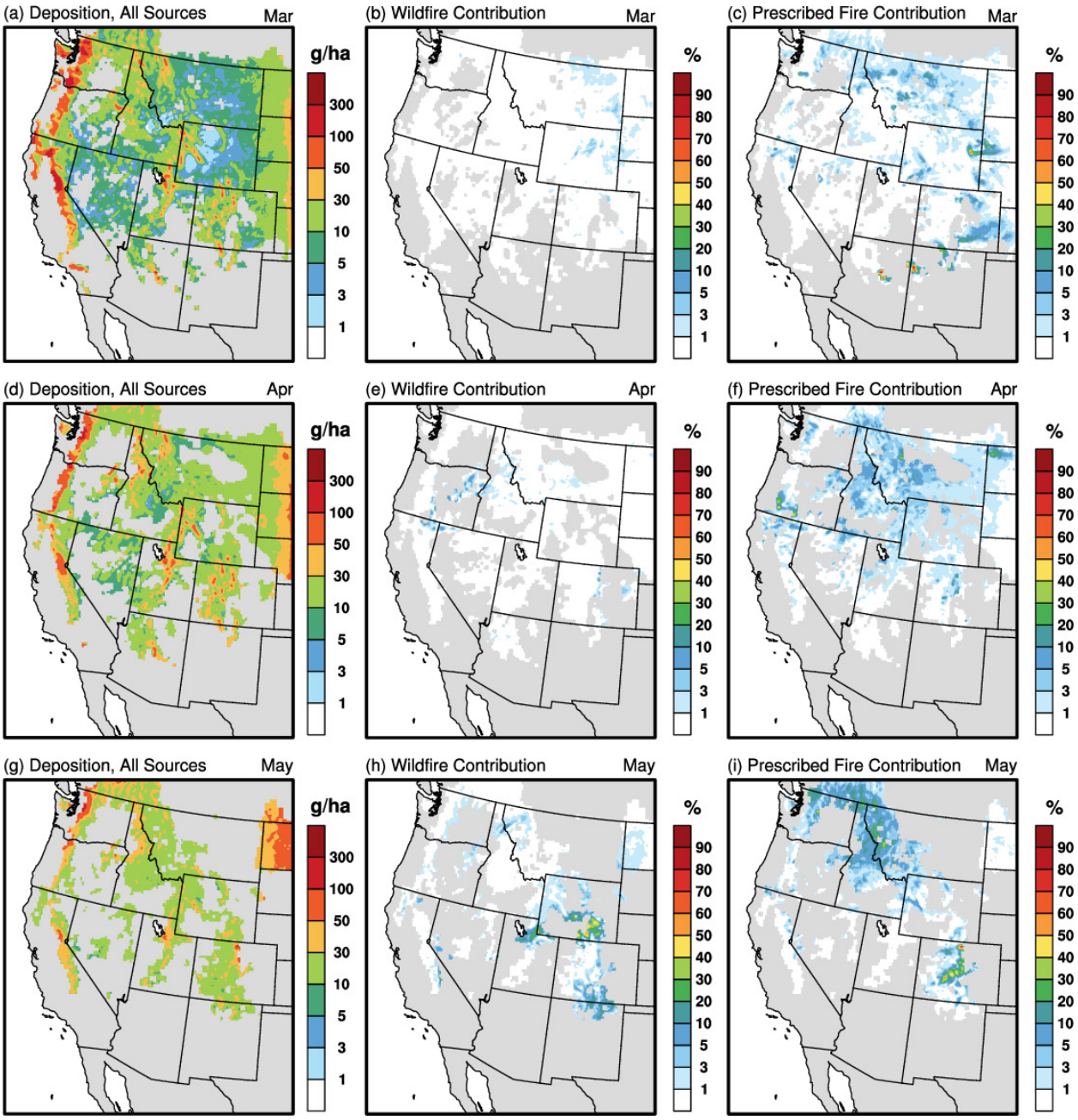

Figure 12. Same as Figure 11, but for spring months.

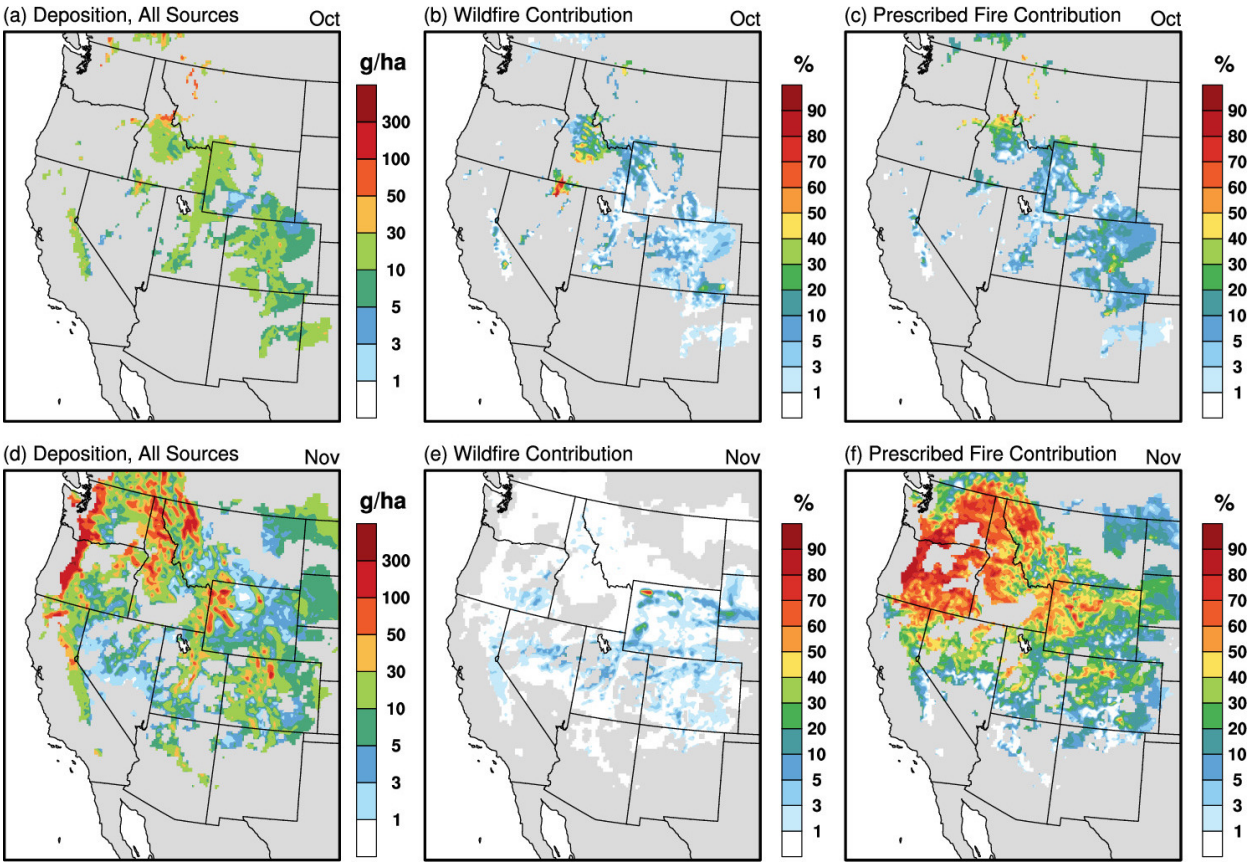

Figure 13. Same as Figure 11, but for October and November.

4. Management Implications

This study is first of its kind in using region scale modeling to assess inter-annual variability of fire emissions on ambient black carbon concentrations and in developing a comprehensive modeling assessment of the contribution of prescribed fires and wildfires to BC deposition to glacier and snow-covered areas in the western United States. Black carbon impacts have been the focus of potential policy discussions in the past 5 years due to the strong impacts of black carbon on climate, particularly when deposited on snowfields and glaciers (US EPA 2012). Should black carbon deposition mitigation be a policy priority, the results of this study may help identify locations and time periods for which black carbon from wildfires and prescribed burning are of particular interest.

Atmospheric concentrations: This work showed that wildland fires' impact on ambient concentrations of black carbon during June to September varied greatly from year to year and by month but that almost every region in the western US was impacted by wildland fires during the 1997-2005 study period. This means reduction in wildland fires has the potential to make significant reduction in ambient black carbon concentrations in the western US. Idaho, western Montana, and northern Wyoming were identified as the regions most impacted by wildland fires while other areas were also significantly impacted.

Glacial areas: This work showed that the non-wildland fire sources dominated annual BC deposition rates to glacial areas, but monthly contributions during summer from wildfires and during fall and winter from prescribed fires can be significant.

Snow covered areas: For lack carbon deposition onto snow-covered surfaces, prescribed fires in Washington, Oregon, Idaho, Wyoming, and Colorado were significant contributors in significant portions of these states during November, when high emissions from prescribed fires coincided with large snow-covered areas. Contributions from wildfires were generally negligible outside of October and May because of the lack for snow surfaces during the warmer months when wildfires were more active. Managers and policy makers can use the spatial maps provided by this report to identify locations and months for mitigation efforts if such efforts are determined to be a priority.

5. Relationship to other recent findings and ongoing work on this topic

The goal of the project was to assess the contributions of wildland fires to ambient black carbon concentrations and depositions to glacier and snow-covered areas in the western US. Due to the highly variable nature of wildfires, both in fire occurrences on the landscape and the high spatial and temporal variability of fuels, consumption, and emissions, the impact of wildfire emissions varies significantly over the period of the wildfire season as well as inter-annually. The comprehensive simulations performed in this work highlighted the significant role of wildland fires on BC concentrations over the western US, their inter-annual variability, and the seasonal trends in contributions of wildfires vs. prescribed burning. While the role of BC on snow albedo has been highlighted in the literature, we believe this is the first modeling study to assess the role of wildland fires on BC deposition to glaciers and snow-covered areas in the western US.

Other studies have suggested climate change climate change has already caused an increase in wildfire activity in the western US and have predicted increased wildfire risk and area burned for in the future. The projected increase in fire activity in the context of expected reduction in black carbon emissions from fossil fuel indicates increased contributions from wildland fires in the future. This work can be used as the basis for comparison for other studies that focus on historical, current, or projected contributions of wildland fires. Examples of projects on future contributions of fires include JFSP Projects #13-1-01-4 and # 13-1-01-16 and projects soon to be funded by the EPA on “Particulate Matter and Related Pollutants in a Changing World” (http://cfpub.epa.gov/ncer_abstracts/index.cfm/fuseaction/display.rfatext/rfa_id/594).

6. Future Work

While the modeling assessment in this work is an important step for determining the contributions of wild and prescribed fires to ambient black carbon concentrations and to deposition onto glacier and snow-covered surfaces, there are several areas where the assessment could be improved.

The meteorological simulations using WRF exhibited cold biases and errors in precipitation (see Appendix A). Future work using different physics options of the WRF model and smaller grid cells may help to improve model performance. The latter may be useful because the western US is characterized by complex terrain. With respect to modeling the transport of black carbon and deposition, plume-rise was likely a major source of modeling errors. As with most regional modeling studies, a plume-rise algorithm based on power plant emissions was applied to fire

emissions. Other studies, including our evaluation in Herron-Thorpe et al. (2013), indicate that such simplification of fire plume behavior is a major source of model error.

The detailed analysis done for the 2011 case, involving both wildfires and prescribed fires, should be extended for multiple years. Doing so would help account for both inter-annual variability in fire activity and also in snowpack extent, allowing for analysis of confounding factors such as inter-annual climate variability (e.g., El Niño is often correlated with warmer and drier winters and thus less snow). To do so, a detailed long-term fire emissions inventory that incorporates both wildfires and prescribed burns needs to be developed. This can follow the work done for the 2011 National Emissions Inventory, and include improvements from lessons learned from that effort as well as current projects (e.g. JFSP Project #12-1-07-2). Some of these improvements are being incorporated into the 2014 NEI, but the emissions inventory needs to extend these efforts to a continuous, multi-year inventory and not an every 3 year analysis.

This study assessed the contribution of wildland fires to deposition on a monthly basis. However, the relatively timing of snow and BC deposition is an important determinant if BC will actual affect snow albedo. For example, BC deposited before the start of a snowstorm may be completely buried by the snow and have no impact on surface snow albedo. Future work should refine the assessment at a daily time scale.

Quantifying the deposition rates is only a first step in evaluating impact of wildland fire emissions on snow albedo, radiative forcing, hydrological cycles, and ultimately climate. For example, Qian et al. (2009) investigated how BC-induced snow albedo change affected snowpack and hydrological cycle in the western US by modeling the effect of BC on snow albedo and coupling the results to a meteorological model. However, Qian et al. (2009) did not consider black carbon from fires, which our study suggested contributed significantly to the deposition in November of 2011. A similar modeling assessment as that of Qian et al. (2009) but that also evaluated the contributions from wildfires, prescribed fires, and other sources is an obvious next step.

7. Deliverables

Proposed	Description	Status
Webpage setup	Project webpage set up and posted publicly	Completed; http://lar.wsu.edu/firebc/
Preliminary report #1	Inter-annual variability of fire impact	Completed. Results are now included in this final report. Note that the analysis had been extended beyond the original proposed simulation periods to include September 1998-2005 and June-September of 1997 because wildfires were active September and 1997 was the biggest El Niño events in last 60 years.
Preliminary report #2	Seasonality of fire impact	Completed. Results are now included in this final report. Note that we replaced the proposed 36-km simulations with12-km simulations because higher resolution is better suited for the mountainous terrain of the western US.
Presentation at the Joint fire and fuels management conference	Conference attended by land management, air quality, and decision making communities	Substituted for the NW-AIRQUEST annual meeting.
Workshops and Technical Conferences	Presentations at AGU & AMS Conferences and other appropriate workshops	Completed: AGU 2013, AAAR 2014
Peer-reviewed article 1	Impact of fire emissions on BC concentrations	In prep
Peer-reviewed article 2	Impact of fire emissions on BC deposition rates	In prep
Compiled modeled fire emissions	Contribution to SEMIP	Completed. In addition, the PI served on the expert panel to the North American Black Carbon Emissions Estimation Guidelines prepared by the Eastern Research Group, Inc. for the Commission for Environmental Cooperation
JFSP final report	Final report to the JFSP describing the results of the project and deliverables	Completed.

List of Presentations

Chung, S.H., Gonzalez-Abraham, R., Lamb, B.K., Larkin, S., Strand, T., and O'Neill, Modeling study of the contribution of wildfires to ambient $PM_{2.5}$ and black carbon Concentrations. *NW-AIRQUEST Annual Meeting*, Boise, ID, June 2014.

Chung, S.H., Gonzalez-Abraham, R., Lamb, B.K., Larkin, S., Strand, T., and O'Neill, Modeling study of the contribution of wildfires to ambient $PM_{2.5}$ and black carbon Concentrations. *NW-AIRQUEST Quarterly Meeting*, Seattle, WA, February 2015.

Chung, S.H., Gonzalez-Abraham, R., Lamb, B.K., Larkin, S., Strand, T., and O'Neill, Modeling study of the contribution of wildfires to ambient black carbon Concentrations. *American Geophysical Meeting Annual Fall Meeting*, San Francisco, CA, December 2013.

Wiedinmyer, C., Chung, S.H., Yokelson, R.J., McDonald-Buller E., Oda T., Elvidge C., Emmons, L., Orlando J., Constraining emissions from open burning sources and their atmospheric impacts, *American Association for Aerosol Research Annual Conference*, Orlando, Florida, October 2014.

References

Anderson G.K., D.V. Sandberg and R.A. Norheim (2004), Fire emissions production simulator (FEPS) user's guide. Available at http://www.fs.fed.us/fera/feps

Avise, J., R. Gonzales Abraham, S. H. Chung, J. Chen, B. Lamb, E. P. Salathé, E. P., Y. Zhang, C. G. Nolte, D. H. Loughlin, A. Guenther, C. Wiedinmyer, and T. Duhl (2012), Evaluating the effects of climate change on summertime ozone using a relative response factor approach for policymakers, *J. Air Waste Manag. Assoc.*, 62(9), 1061–1074, doi:10.1080/10962247.2012.696531.

Barbero, R., Abatzoglou, J.T., Larkin, N.K., Kolden, C.A., and Stocks, B. (2015). Climate change presents increased potential for very large fires in the contiguous United States. *Int. J. Wildland Fire,* DOI 10.1071/WF15083.

Barsanti, K. C., Carlton, A. G. and Chung, S. H. (2013), Analyzing experimental data and model parameters: implications for predictions of SOA using chemical transport models, *Atmos. Chem. Phys.*, 13(23), 12073–12088, doi:10.5194/acp-13-12073-2013.

Bond, TC (2007), Can warming particles enter global climate discussions? *Environ. Res. Lett.*, 2(4), 045030, doi:10.1088/1748-9326/2/4/045030.

Boylan, J. W. and Russell, A. G. (2006), PM and light extinction model performance metrics, goals, and criteria for three-dimensional air quality models, *Atmos. Environ.*, 40(26), 4946–4959, doi:10.1016/j.atmonsenv.2005.09.087.

Byun, D., and K. L. Schere (2006), Review of the governing equations, computational algorithms, and other components of the models-3 Community Multiscale Air Quality (CMAQ) modeling system, *Appl. Mech. Rev.*, 59(1-6), 51–77, doi:10.1115/1.2128636.

Carlton, A. G., Bhave, P. V., Napelenok, S. L., Edney, E. D., Sarwar, G., Pinder, R. W., Pouliot, G. A. and Houyoux, M. (2010), Model representation of secondary organic aerosol in CMAQv4.7, *Environ. Sci. Technol.*, 44(22), 8553–8560, doi:10.1021/es100636q.

Carroll, T., D. Cline, G. Fall, A. Nilsson, L. Li, and A. Rost (2001), NOHRSC Operations and the Simulation of Snow Cover Properties for the Conterminous U.S., *Proceedings of the 69th Annual Meeting of the Western Snow Conference,* pp. 1-14.

Chen, J., J. Vaughan, J. Avise, S. O'Neill, and B. Lamb (2008), Enhancement and evaluation of the AIRPACT ozone and PM2.5 forecast system for the Pacific Northwest, *J. Geophys. Res.*, *113*(D14), D14305, doi:10.1029/2007JD009554.

Emmons, L. K., S. Walters, P. G. Hess, J-.F. Lamarque, G. G. Pfister, D. Fillmore, C. Granier, A. Guenther, D. Kinnison, T. Laepple, J. Orlando, X. Tie, G. Tyndall, C. Wiedinmyer, S. L. Baughcum, S. Kloster (2010), Description and evaluation of the Model for Ozone and Related chemical Tracers, version 4 (MOZART-4), *Geosc. Model Devel.*, 3(1), 43–67, doi:10.5194/gmd-3-43-2010.

Herron-Thorpe, F.L., Mount, G.H., Emmons, L.K., Lamb, B.K., Jaffe, D.A., Wigder, N.L., Chung, S.H., Zhang, R., Woelfle, M.D., Leung, F.-Y., Vaughan, J.K. (2014), Regional model simulations of wildfires in the Pacific Northwest evaluated with surface measurements and satellite retrievals during the summers of 2007 and 2008, *Atmospheric Chemistry and Physics*, 14(22), 12533–12551, doi:10.5194/acp-14-12533-2014.

GLIMS and NSIDC (2005), Global Land Ice Measurements from Space glacier database. Compiled and made available by the international GLIMS community and the National Snow and Ice Data Center, Boulder CO, U.S.A. DOI:10.7265/N5V98602

Gonzalez-Abraham, R., J.C. Avise, S. H. Chung, B. K. Lamb, E. P. Salathé, C. Nolte, D. Loughlin, A. Guenther, C. Wiedinmyer, T. Duhl, Y. Zhang and D. G. Streets (2015), The effects of global change upon United States Air Quality, *Atmos. Chem. Phys.,* accepted.

Guenther, A., T. Karl, P. Harley, C. Wiedinmyer, P. I. Palmer, and C. Geron (2006), Estimates of global terrestrial isoprene emissions using MEGAN (Model of Emissions of Gases and Aerosols from Nature), *Atmos. Chem. Phys.*, 6(11), 3181–3210, doi:10.5194/acp-6-3181-2006.

Jaffe, D., Hafner, W., Chand, D., Westerling, A. and Spracklen, D. (2008), Interannual variations in $PM_{2.5}$ due to wildfires in the Western United States, *Environ. Sci. Technol.*, 42(8), 2812–2818, doi:10.1021/es702755v.

Jacobson, M. Z. (2004), Climate response of fossil fuel and biofuel soot, accounting for soot's feedback to snow and sea ice albedo and emissivity, *J. Geophys. Res.*, 109(D21), doi:10.1029/2004JD004945.

Hughes, P. Y., E. H. Mason, T. R. Karl, and W. A. Brower (1992), United States Historical Climatology Network Daily Temperature and Precipitation Data. ORNL/CDIAC-50, NDP-042. Carbon Dioxide Information Analysis Center, Oak Ridge National Laboratory, U.S. Department of Energy, Oak Ridge, Tennessee.

Kanamitsu, M., W. Ebisuzaki, J. Woollen, S.-K. Yang, J. J. Hnilo, M. Fiorino, and G. L. Potter, (2002), NCEP–DOE AMIP-II Reanalysis (R-2). *Bull. Amer. Meteor. Soc.*, 83, 1631–1643.

Kemball-Cook, S., Y. Jia, C. Emery, and R. Morris (2005), Alaska MM5 Modeling for the 2002 Annual Period to Support Visibility Modeling. Prepared for the Western Regional Air Partnership, by ENVIRON International Corp., Novato, CA. Available at: http://pah.cert.ucr.edu/aqm/308/docs/alaska/Alaska_MM5_DraftReport_Sept05.pdf

Larkin N. K., S. M. Raffuse and T. M. (2014), Wildland fire emissions, carbon, and climate: U.S. emissions inventories. Forest Ecology and Management, 317, 61-69.

Larkin, N. K, S. M. O'Neill, R. Solomon, S. Raffuse, T. Strand, D. C. Sullivan, C. Krull, M. Rorig, J. L. Peterson, and S. A. Ferguson (2009), The BlueSky smoke modeling framework, *Intl. J. Wildland Fire*, 18(8), 906-920, doi:10.1071/WF07086.

McKenzie, D., C. L. Raymond, L.-K. B. Kellogg, R. A. Norheim, A. G. Andreu, A. C. Bayard, K. E. Kopper, E. Elman (2007), Mapping fuels at multiple scales: landscape application of the Fuel Characteristic Classification System, *Canadian Journal of Forest Research*, 37, 12, 2421-2437.

McNally, D. E., (2009), 12 km MM5 Performance Goals. Presentation to the Ad-Hoc Meteorology Group. June 25, 2009. Available at: http://www.epa.gov/scram001/adhoc/mcnally2009.pdf

Mesinger, F. et al. (2006), North American Regional Reanalysis, *Bull. Amer. Meteor. Soc.*, *87*(3), 343–360, doi:10.1175/BAMS-87-3-343.

National Operational Hydrologic Remote Sensing Center (2004), Snow Data Assimilation System (SNODAS) Data Products at NSIDC, Boulder, Colorado USA: National Snow and Ice Data Center. http://dx.doi.org/10.7265/N5TB14TC

Otte, T. L., and J. E. Pleim (2010), The Meteorology-Chemistry Interface Processor (MCIP) for the CMAQ modeling system: updates through MCIPv3.4.1, *Geosci. Model Devel.*, *3*, 243–256, doi:10.5194/gmd-3-243-2010.

Prichard S.L., R. D. Ottmar, and G. K. Anderson (2006), Consume 3.0 user's guide. General Technical Report prepared by the USDA Forest Service, Pacific Northwest Research Station, Seattle, WA, PNW-GTR-304. Available at http://www.fs.fed.us/pnw/fera/research/smoke/consume/consume30_users_guide.pdf.

Qian, Y., Gustafson, W. I., Leung, L. R. and Ghan, S. J. (2009), Effects of soot-induced snow albedo change on snowpack and hydrological cycle in western United States based on Weather Research and Forecasting chemistry and regional climate simulations, *J. Geophys. Res.*, 114, doi:10.1029/2008JD011039.

Raffuse S. M., N. K. Larkin, S.-M. Huang, Y. Du, S. Reid, Development of the wildland fire portion of the 2011 National Emissions Inventory, *J. Air Waste Management Association*, in review.

Rasmusson, E.M. and Wallace, J.M. (1983). Meteorological Aspects of the El-Nino Southern Oscillation. Science, 222(4629): 1195-1202.

Reynolds, R.W., N.A. Rayner, T.M. Smith, D.C. Stokes, and W. Wang (2002), An improved in situ and satellite SST analysis for climate. *J. Climate*, 15, 1609-1625.

Salathé, E. P., L. R. Leung, Y. Qian, and Y. Zhang, Y. (2010), Regional climate model projections for the State of Washington, *Climatic Change*, 102(1-2), 51–75, doi:10.1007/s10584-010-9849-y.

Skamarock, W. C., J. B. Klemp, J. Dudhia, D. O. Gill, D. M. Barker, M. G. Duda, X.-Y. Huang, W. Wang, and J. G. Powers (2008), A Description of the Advanced Research WRF Version 3. NCAR/TN–475+STR. Boulder, Colorado: National Center for Atmospheric Research.

Sullivan, D. C., S. M. Raffuse, D. A. Pryden, K. J. Craig, S. B. Reid, N. J. M. Wheeler, L. R. Chinkin, N. K. Larkin, R. Solomon, and T. Strand (2008), Development and applications of systems for modeling emissions and smoke from fires: the BlueSky smoke modeling framework and SMARTFIRE: 17th International Emissions Inventory Conference, Portland, OR, June 2, 2008.

U.S. Environmental Protection Agency (2012) Report to Congress on black carbon. Report prepared by the Office of Air Quality Planning and Standards, Office of Atmospheric Programs, Office of Radiation and Indoor Air, Office of Research and Development, and Office of Transportation and Air Quality, Research Triangle Park, NC, EPA-450/R-12-001, March. Available on the Internet at http://www.epa.gov/blackcarbon/.

Vukovich, J. and T. Pierce (2002), The Implementation of BEIS3 within the SMOKE Modeling Framework, in Proceedings of the 11th International Emissions Inventory Conference, Atlanta, Georgia, April 15-18, 2002. (Available online: www.epa.gov/ttn/chief/conference/ei11/modeling/vukovich.pdf).

Zhang, Y., V. Dulière, P. W. Mote, and E. P. Salathé Jr. (200), Evaluation of WRF and HadRM mesoscale climate simulations over the U.S. Pacific Northwest, *J. Climate*, 22(20), 5511–5526, doi:10.1175/2009JCLI2875.1.

Appendix A. Model Evaluation

A critical part of modeling air quality is the meteorological fields used to drive the chemical transport model. This is true for air quality forecasting or hindcast simulations as well as in climate change studies. In climate change studies, for consistent comparisons between future projections and historical time periods, global climate model results instead of reanalysis fields are used as initial and boundary conditions to drive regional climate models such as WRF even for the historical periods. In Avise et al. (2012) and Gonzalez-Abraham et al. (2015), results from the ECHAM5 global climate model were used to drive WRF simulations to evaluate how climate change impact regional air quality in the US. Here, WRF results from those studies and 36-km CONUS and 12-km western US WRF simulations performed for this study are compared against observed daily maximum temperature and precipitation data for 1201 stations in the US Historical Climate Network (Hughes et al. 1992); the HCN data were obtained from the Carbon Dioxide Information Analysis Center (CDIAC) (http://cdiac.ornl.gov/epubs/ndp/ushcn/ushcn.html). In addition, for BC concentrations, data from the Interagency Monitoring of Protected Visual Environments (IMPROVE) network (obtained from http://views.cira.colostate.edu/fed/DataWizard/Default.aspx) were used. The following metrics were used for the evaluations:

Mean Fractional Bias (%)	$\mathrm{FB} = \frac{1}{N}\sum_{i=1}^{N} \frac{(C_\mathrm{m} - C_\mathrm{o})}{\frac{C_\mathrm{m} + C_\mathrm{o}}{2}}$
Mean Fractional Error (%)	$\mathrm{FE} = \frac{1}{N}\sum_{i=1}^{N} \frac{\lvert C_\mathrm{m} - C_\mathrm{o}\rvert}{\frac{C_\mathrm{m} + C_\mathrm{o}}{2}}$
Mean Bias	$\mathrm{MB} = \frac{1}{N}\sum_{i=1}^{N} (C_\mathrm{m} - C_\mathrm{o})$
Mean Error	$\mathrm{ME} = \frac{1}{N}\sum_{i=1}^{N} \lvert C_\mathrm{m} - C_o\rvert$
Correlation Coefficient	$r = \frac{\sum_{i=1}^{N}(C_\mathrm{m} - \overline{C_\mathrm{m}})(C_o - \overline{C_o})}{\left[\sum_{i=1}^{N} (C_\mathrm{m} - \overline{C_\mathrm{m}})^2 \sum_{i=1}^{N} (C_\mathrm{o} - \overline{C_\mathrm{o}})^2\right]^{1/2}}$

where C_o and C_m are observed and modeled values (concentrations, temperature, or precipitation) and *N* is the number of paired data points.

A.1 Simulation Period #1 – 1997-2005 June-September CONUS

A.1.1 Meteorological Evaluation

For a climatological evaluation, Figure A-1ab shows the distributions of daily maximum temperature (T_max) and monthly total precipitation for June, July, and August for the two sets of WRF results and observations. The figure is based on observations and reanalysis-drive WRF simulations for 1997-2005 and five selected years in 1996-2005 in the ECHAM5-driven WRF simulations. In terms of climatology, the reanalysis-driven WRF performs similarly or better in the Central, the South, and the Midwest regions, but performed worse than the ECHAM5-driven WRF simulation and showed cold biases in T_max for the other regions. Both sets of WRF simulations show cold biases in daily T_max for the Pacific Northwest region, consistent with the results of Zhang et al. (2009) and Salathé et al (2010); they indicated that for the reanalysis-driven WRF simulation the cold biases in T_max is introduced by the DOE/NCEP R-2 reanalysis data. WRF simulation is able to correct the cold T_max biases but only partially. These cold biases may potentially lead to model underestimation of total $PM_{2.5}$ (less photochemistry and oxidation of semi-volatile organics that leads to secondary organic aerosol formation). Linear regression

analysis on reanalysis-driven WRF versus observed daily maximum temperatures (T_{max}) gives r^2 of 0.57 to 0.66, depending on the region, indicating that the WRF results capture most of the observed day-to-day variations in T_{max}; mean biases range from 2.16 to 4.17 K and mean errors range from 0.9 to -3.2 K (Figure A-1c). For comparison, benchmarks suggested for acceptable model performance include a mean bias < ±1 K to <± 2 K and a mean error <± 3 K to ± 3.5 K (Kemball-Cook et al., 2005; McNally et al., 2009). Therefore, future work should include improving model performances in the Northwest and Southwest.

For monthly precipitation, reanalysis-driven WRF performs better than the ECHAM5-driven WRF simulations in terms of capturing the median values, except for the Midwest and the Southeast. In the regions for which the model medians match those of observations, the model peak values are less than observed, which is expected because of smoothing introduced by the use of a coarse grid. For precipitation, at daily time scale, the correlation between reanalysis-drive WRF and observed precipitation is low (not shown), indicative of the difficulty in predicting precipitation at the right location at the right time. On monthly time scale, correlations range from r^2= 0.19 to 0.55 and mean errors range from -0.4 to 3 cm, depending on the region (Figure A-1d).

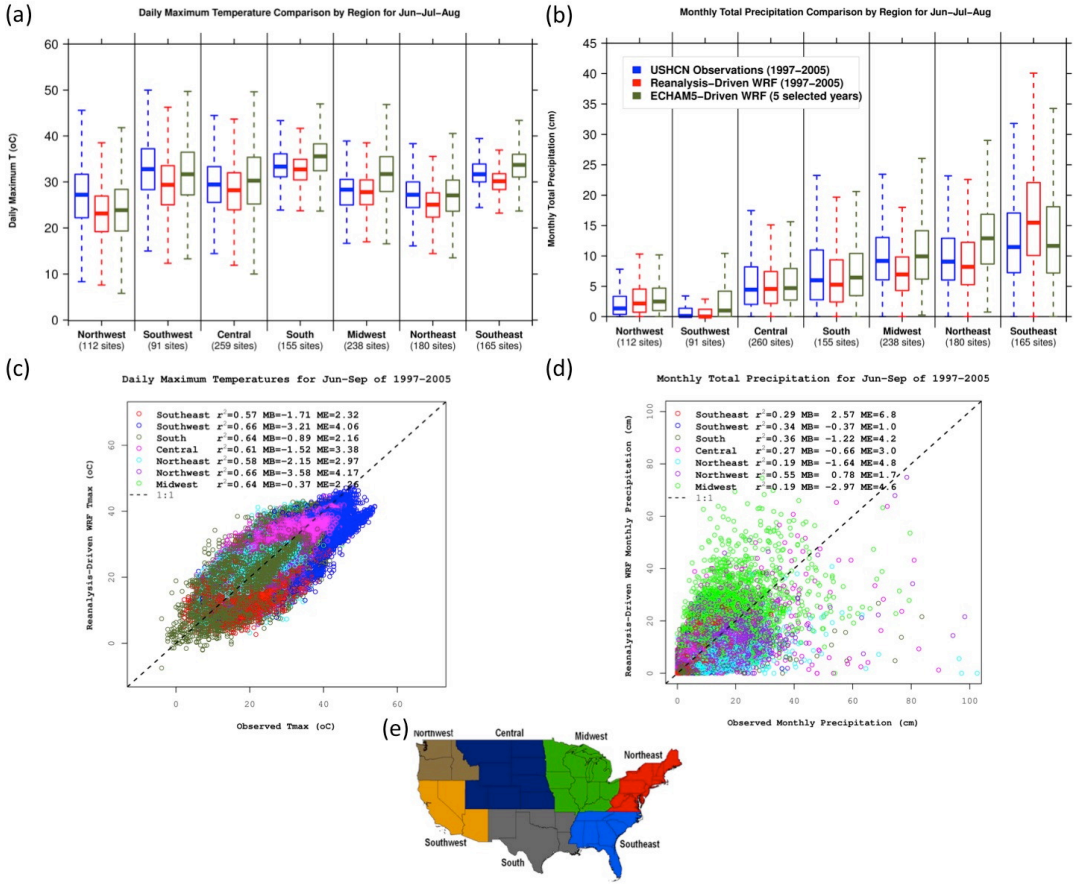

Figure A-1. Meteorological evaluations for the 36-km CONUS WRF simulation. The left panel shows daily maximum temperature (°C); the right panel shows monthly precipitation (cm). The top panel shows the climatology for summer (Jun, Jul, and Aug) based on data from the US Historical Climate Network (USHCN) (Hughes et al. 1992), reanalysis-driven 1997-2005 WRF simulations performed for this study, and ECHAM5-driven WRF simulations used in Avise et al. (2012) and Gonzalez-Abraham et al. (2015); the whiskers indicate the median, 25th and 75th percentiles, and 1.5 times the interquartile range. Scatter plots in the bottom panel include USHCN data and reanalysis-driven WRF results for the months of Jun, Jul, Aug, and Sep for 1997-2005.

A.1.2 Evaluation of Modeled BC Concentrations

Figure A-2 and Figure A-3 show the evaluation of modeled 24-hour BC concentrations using observed data at 103 IMPROVE sites in the western US for the June-September, 1997-2005 36-km CMAQ simulation that included fire emissions. Even though the simulation was for CONUS, the analysis focused on the western US where wildland fires are most active. Note that observational data were not available for all sites for the entire modeling time period. In Figure A-1 and Figure A-2, model results were extracted only for the dates and sites for which IMPROVE data were available. On average, when the results were aggregated by regions as defined in Figure A-3, the model under-predicted BC concentrations, with mean fractional bias ranging from -30% to -103% (Figure A-3) and mean biases ranging from -0.8 to -0.38 μg m^{-3} (not shown), depending on the region and month. One possible reason for the general underprediction is missing emission sources. Other possible reasons include that BC was being deposited too fast or being too diluted due to the coarse grid cells used.

In Figure A-2, the mean fractional bias and mean fraction error for the 103 IMPROVE sites are shown along with the performance criteria and performance goal specified by Boylan and Russell (2006). Performance goals are defined as the level of accuracy that is considered to be close to the best a model can be expected to achieve; and performance criteria is defined as the level of accuracy that is considered to be acceptable for modeling applications. Model performance at only two of the 103 sites did not satisfy the mean fractional error performance criteria (Figure A-2b). The two sites were the Salmon National Forest site in Idaho and the South Lake Tahoe in California; there were only three 24-hour BC data points available for these two sites. In addition to these two sites, model performance also did not meet the mean fractional bias criteria for the Glacier National Park site in Montana (Figure A-2a). In summary, the model performance for 100 of the 103 sites met the performance criteria and for 99 of these sites the model met the performance goal.

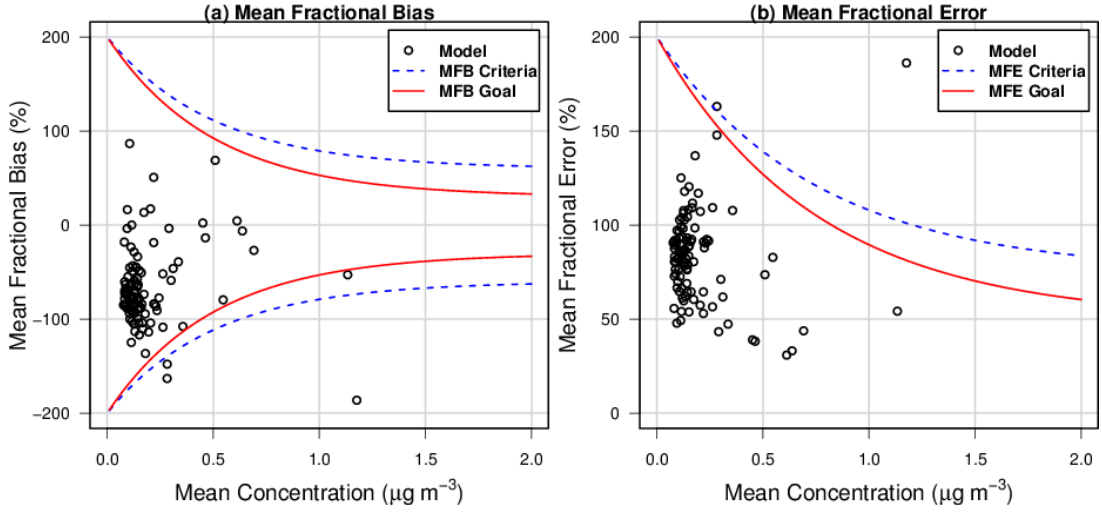

Figure A-2. (a) Mean fractional bias and (b) mean fractional error for 24-hour BC concentrations compared to the performance criteria and goal of Boylan and Russell (2006) for the 36-km June-September 1997-2005 simulation. Each point represents the mean fraction bias or mean fraction error of all data one of the 103 IMPROVE sites.

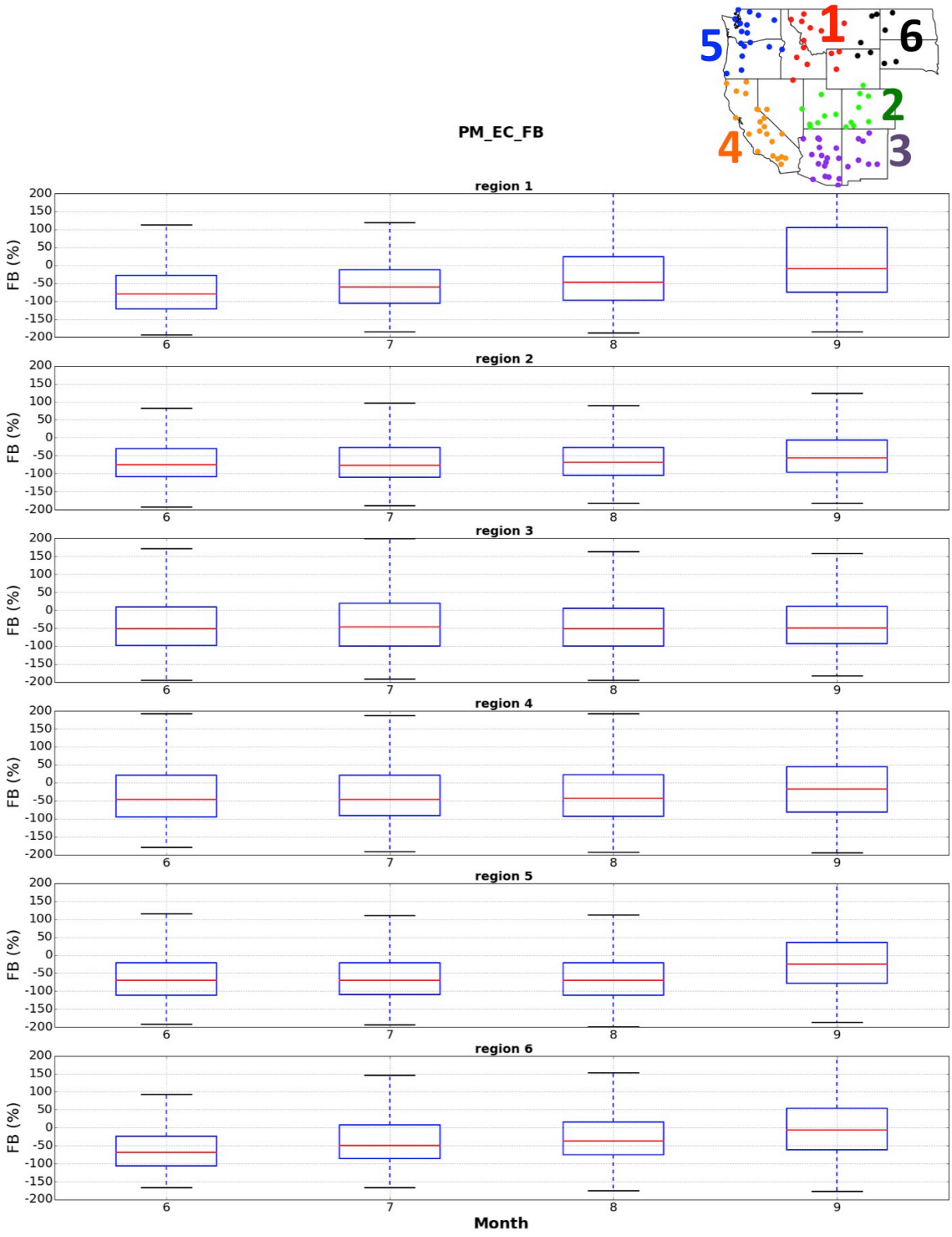

Figure A-3. Fractional bias of modeled 24-hour BC concentrations compared against observed data at 103 IMPROVE sites in the western US for the June-September 1997-2005 36-km CMAQ simulation that included fire emissions. The whiskers indicate the median, 25th and 75th percentiles, and 1.5 times the interquartile range.

A.2 Simulation Period #2 – 2011 Western U.S.

A.2.1 Meteorological Evaluation

Figure A-4, Figure A-5 and Figure A-6 show comparisons of model results for the 12-km western US WRF simulation with observational data from 360 stations in the US Historical Climate Network (USHCN) (Hughes et al. 1992). Figure A-4a shows that the model performed well in terms of capturing the day-to-day variation in daily maximum temperatures $T_{\max}$, with r^2 ranging from 0.84 to 0.87. However, the model showed a cold bias in daily $T_{\max}$ for all months and regions in the modeling domain (Figure A-5). The mean bias averaged over each region and over the entire year ranged from -2 to -3 K and the mean error ranged from 3.4 to 3.8 K (Figure A-4a). Figure A-4b shows that the model captured most of the variation in monthly total precipitation, with r^2 ranging from 0.39 to 0.73. Averaged over each region and over the entire year, the model mean bias was negative for the Southwest and positive for other regions; however, the model performance varied by month (Figure A-6). Future work should consider different physics options in the WRF model as well as smaller grid cells to correct the cold biases in daily maximum temperatures and to improve precipitation results.

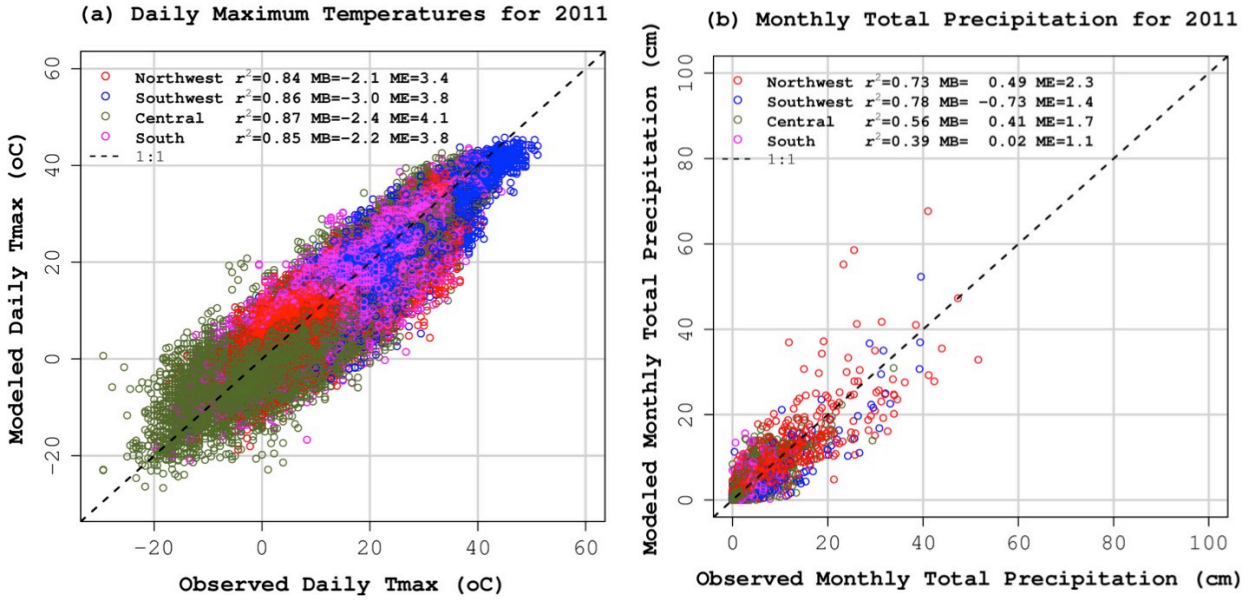

Figure A-4. Scattered plots for modeled vs. observed (a) daily maximum temperatures and (b) monthly total precipitation for the 2011 12-km western US WRF simulation. Observed data were from 360 stations in the US Historical Climate Network (USHCN) (Hughes et al. 1992). The regions are defined in Figure A-1e.

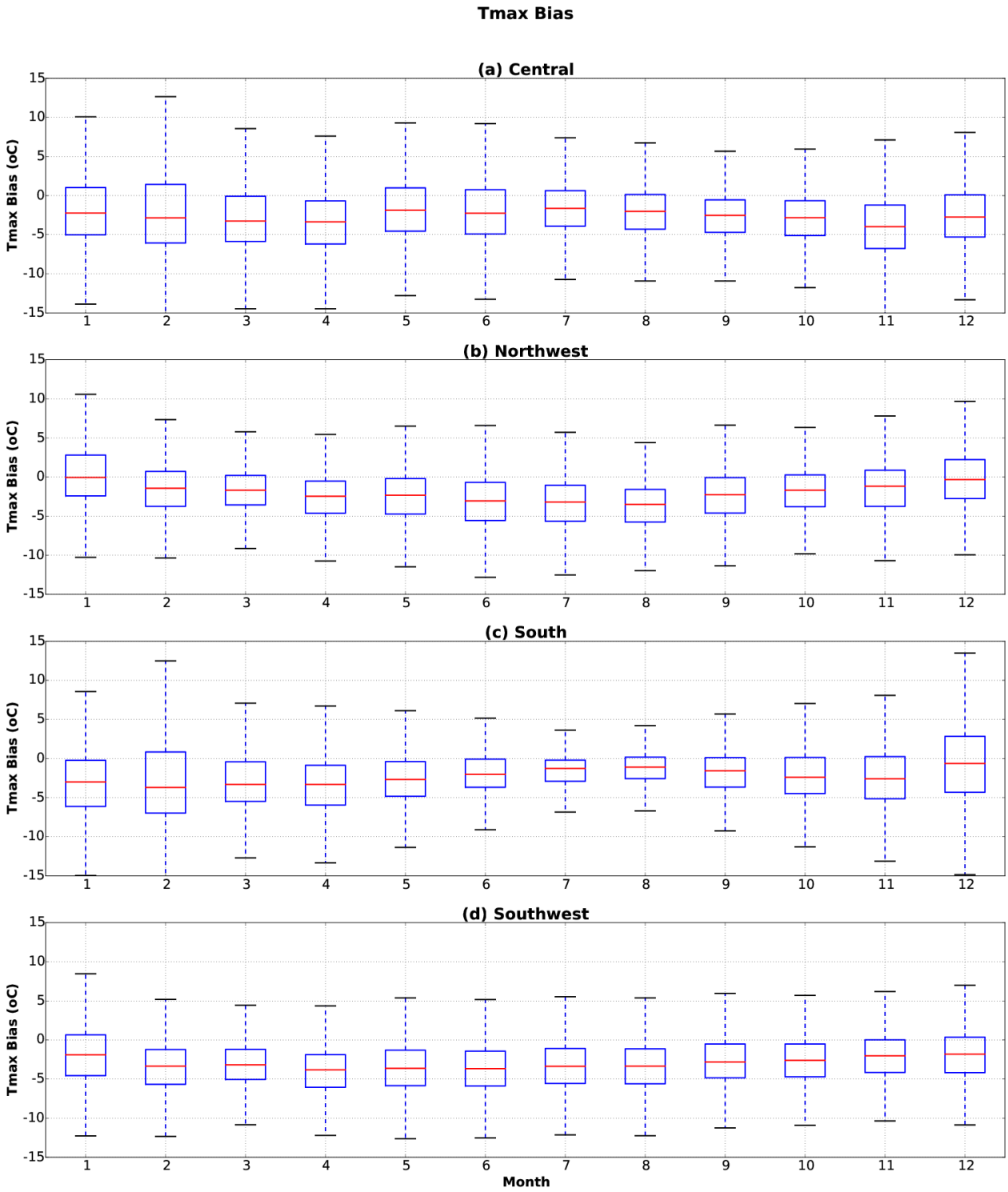

Figure A-5. Model biases in daily T_{max} for the 2011 12-km western US WRF simulation. The whiskers indicate the median, 25th and 75th percentiles, and 1.5 times the interquartile range. Observed data were from 360 stations in the US Historical Climate Network (USHCN) (Hughes et al. 1992). The regions are defined in Figure A-1e.

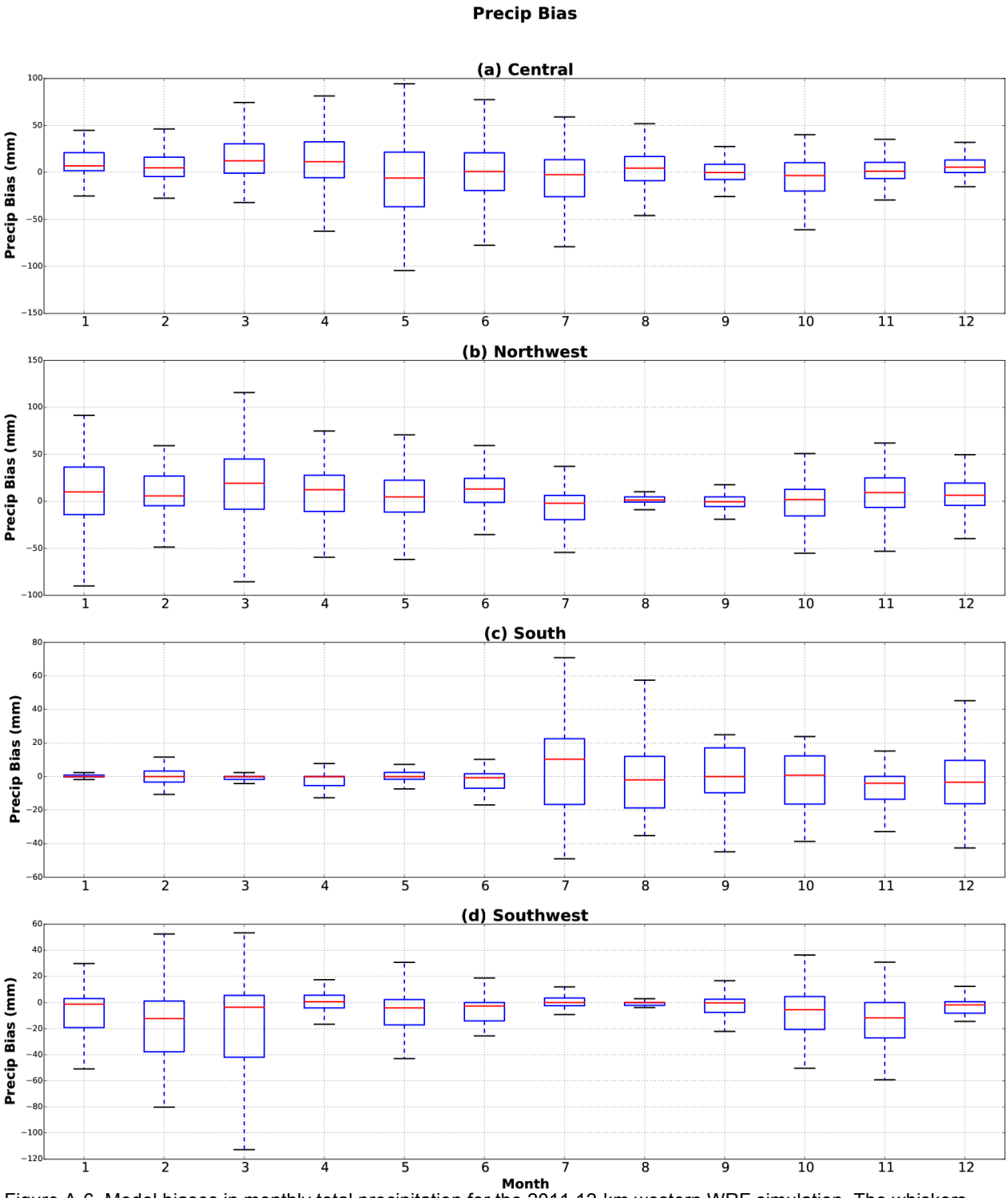

Figure A-6. Model biases in monthly total precipitation for the 2011 12-km western WRF simulation. The whiskers indicate the median, 25th and 75th percentiles, and 1.5 times the interquartile range. Observed data were from 360 stations in the US Historical Climate Network (USHCN) (Hughes et al. 1992). The regions are defined in Figure A-3e.

A.2.2 Evaluation of Modeled BC Concentrations

Figure A-7 and Figure A-8 show the evaluation of modeled 24-hour BC concentrations using observed data at 96 IMPROVE sites in the western US for the 2011 12-km CMAQ simulation that included all emissions in the NEI 2011 inventory. Note that observational data were not available for all sites for the entire modeling time period. In Figure A-7 and Figure A-8, model results were extracted only for the dates and sites for which IMPROVE data were available. Figure A-8 shows the distributions of fractional bias by region and month. On average, the model tended to under-predict BC concentrations for Region 6 (eastern Montana, northwestern Wyoming, and western Dakotas), with November, January, and February being the exceptions. The model tended to over-predict BC concentrations for Region 5 (Washington and Oregon), with May, June, and July being the exceptions. For the other regions, the mean fractional bias (MFB) tended to be lower (more negative or less positive) for spring and higher (more positive or less negative) for late fall and winter. Overall, MFB ranged from -76% to 65% and mean bias ranged from -0.08 to 0.3 $\mu g\ m^{-3}$ (not shown) depending on the region and month.

In Figure A-7, the mean fractional bias (MFB) and mean fraction error (MFE) (averaged over the entire year) for the 96 IMPROVE sites are shown along with the performance criteria and performance goal specified by Boylan and Russell (2006). The model performance did not meet the MFB goal for only 3 of the 96 sites: one site in Seattle and two sites in Phoenix. These three sites were in urban areas and in 2011 had observed annual mean concentrations of 0.75 to 0.82 $\mu g\ m^{-3}$, which were three times higher than all the other sites other than the site at Fresno, California. The model performance met both the MFB and MFE criteria for all sites. The model performance also met the MFE goal for all sites.

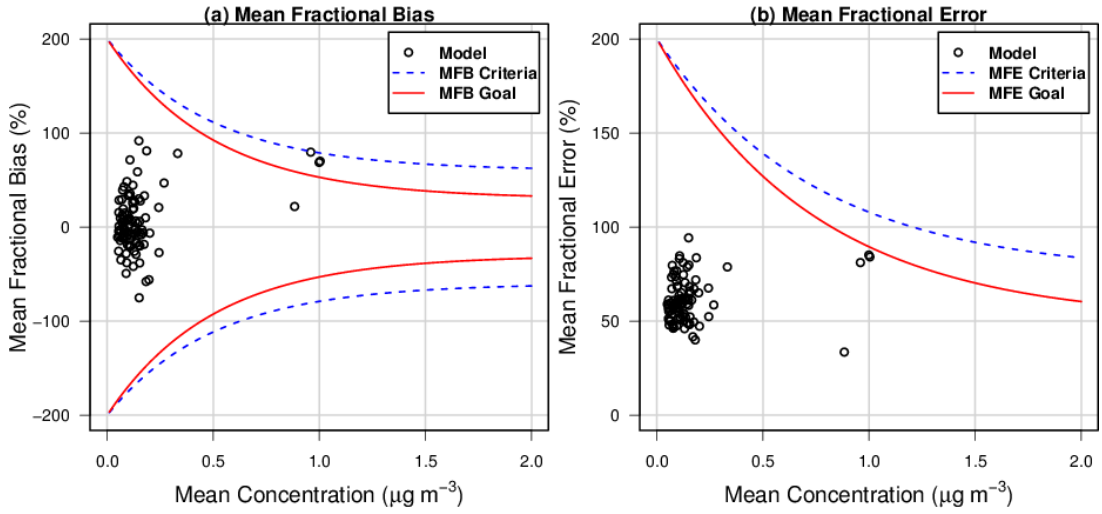

Figure A-7. (a) Mean fractional bias and (b) mean fractional error for 24-hour BC concentrations compared to the performance criteria and goal of Boylan and Russell (2006) for the 2011 12-km western US simulation that included all emissions in the NEI 2011. Each point represents the mean fraction bias or mean fraction error of all data at one of the 96 IMPROVE sites.

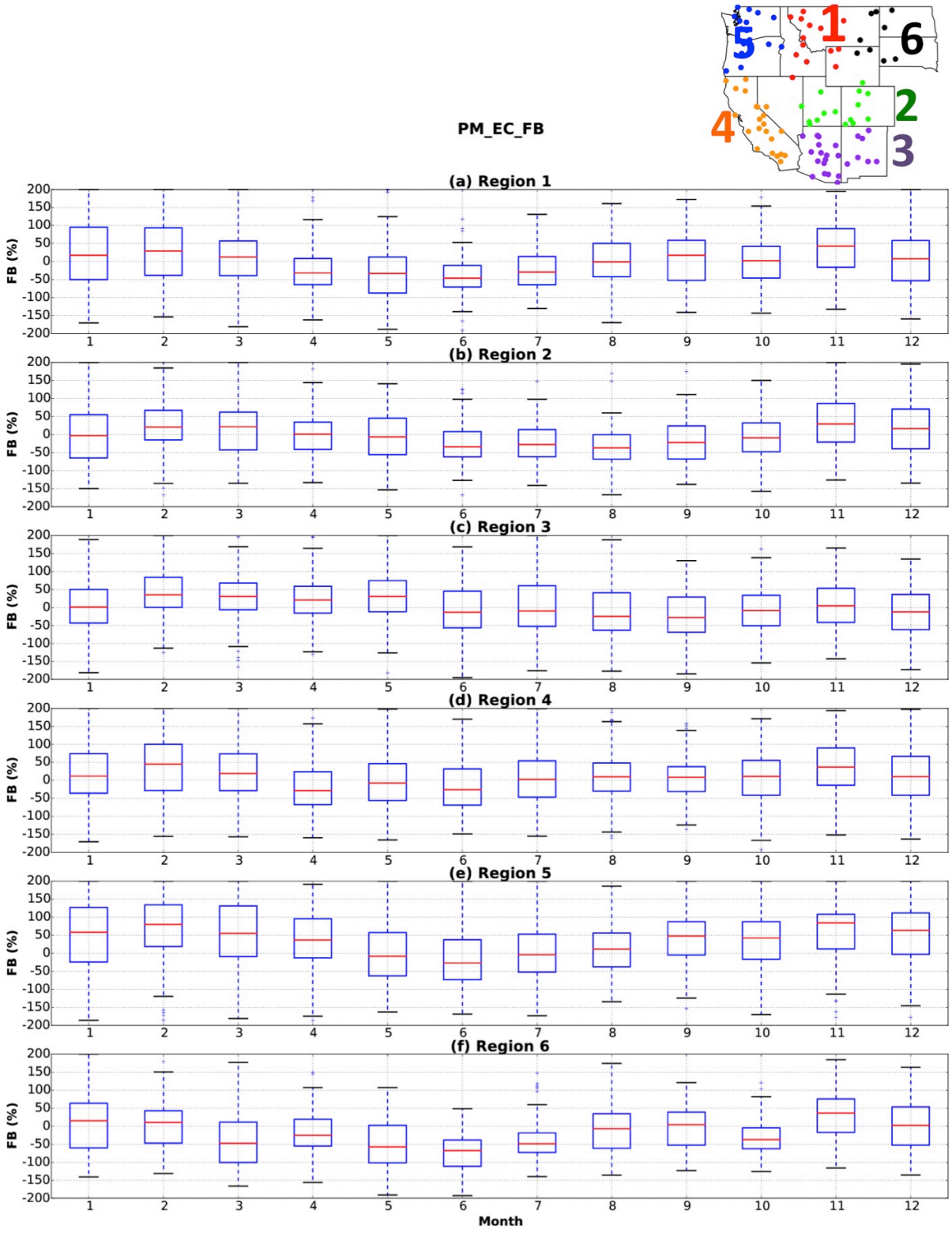

Figure A-8. Fractional bias of modeled 24-hour BC concentrations compared against IMPROVE data for the 2011 12-km western US simulation that included all emissions in the NEI 2011. The whiskers indicate the median, 25th and 75th percentiles, and 1.5 times the interquartile range.